

GNSS-Based Radio Tomographic Studies of the Ionosphere at Different Latitudes

**V. Kunitsyn¹, E. Tereshchenko², E. Andreeva¹,
I. Nesterov¹, Yu. Tumanova¹ and Yu. Fedyunin³**



¹ Faculty of Physics, Lomonosov Moscow State University, Russia

² Polar Geophysical Institute of the Russian Academy of Sciences, Russia

³ Merchant Marine Academy, New York, USA

IES-2015, 11-14 May, 2015, Alexandria, USA

Outline

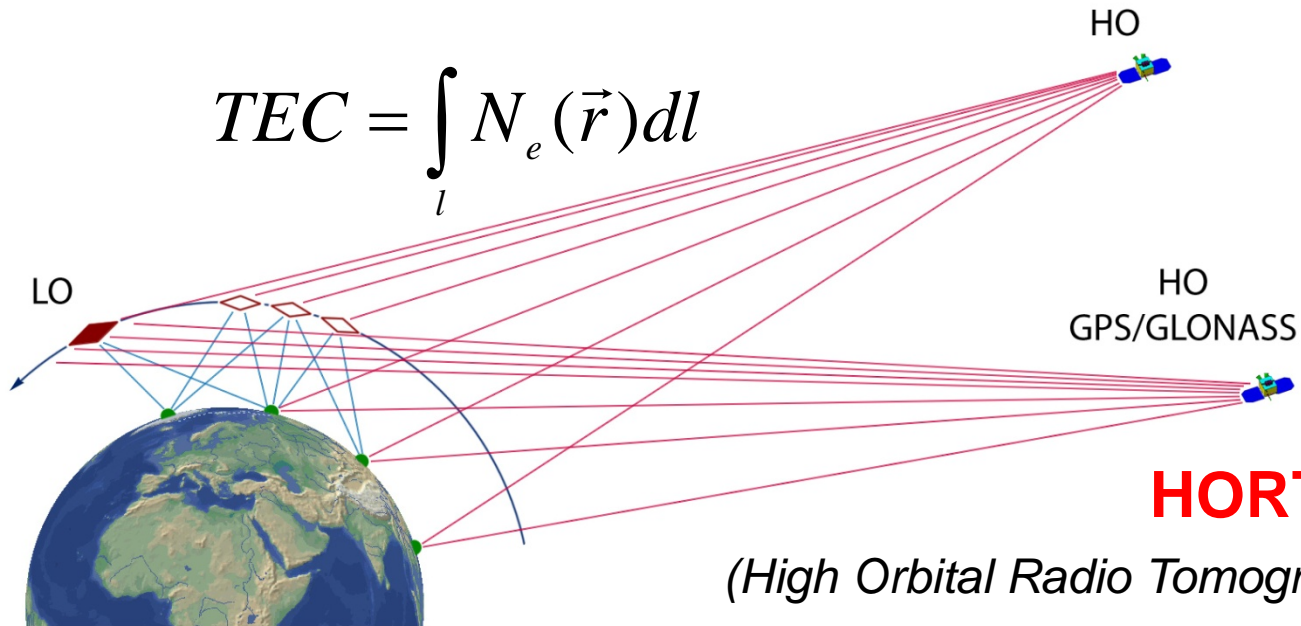
- Global Navigation Satellite Systems (**GNSS**) include:
 - new-generation high orbiting (HO) navigation systems (GPS and GLONASS and under development (Galileo, BeiDou, QZSS systems));
 - and old-generation low orbiting (LO) navigation systems (Tsikada, Transit, etc.).

The GNSS constellations and the networks of ground receivers are suitable for probing the ionosphere along different rays and processing the obtained data by tomographic inversion procedures. The results are obtained by the methods of low orbiting and high orbiting radio tomography (LORT and HORT, respectively).

- We present the examples of tomographic images of the subequatorial, midlatitude, subauroral, and auroral ionosphere in different regions of the world.
- The GNSS RT methods are suitable for imaging the ionospheric disturbances, waves, TIDs caused by different phenomena including the tsunami wave propagation. We analyze the ionospheric disturbances after the strongest Tohoku earthquake in Japan (March 11, 2011).
- The RT reconstructions are compared to the measurements by the ionosondes and Global Ionospheric Maps (GIM).

Methods and Data

$$TEC = \int_l N_e(\vec{r}) dl$$



LORT

(Low Orbital Radio Tomography)

“instantaneous” (~5-10 minutes)
2D RT images of the ionosphere
above the receiving chains

{ the horizontal resolution is **20-30 km**,
and the vertical, **30-40 km**.

The resolution can be improved up to
20-10 km using dense receiving
system and nonlinear RT}

HORT

(High Orbital Radio Tomography)

4D RT images (3 spatial coordinates and
time)

Typical resolution of HORT is about of
100-50 km with a time step **60-20 min**.

resolution can be improved up to **30-50 km**
with a time interval of **30-10 min** in the regions
with dense receiving networks (**West Europe,**
USA, Alaska) and up to **30-10 km & 2min** in
regions with very dense networks (**Japan,**
S. California ...)

Ionospheric Ray Radio Tomography

$$\alpha \lambda r_e \int_L N d\sigma = \Phi = \varphi + \varphi_0,$$

- **Phase RT PT with estimation of initial phase**
(RT using linear integrals, including unknowns initial phase, определение которых является дополнительной задачей)
- **RT using relative phase**
- **Phase-difference RT - RT** using difference of linear integrals on close rays (it's not necessary to determine the initial phase)

Ionospheric Ray Radio Tomography

$$\alpha \lambda r_e \int_L N d\sigma = \Phi = \varphi + \varphi_0, \quad \text{PN} = \Phi + \xi$$

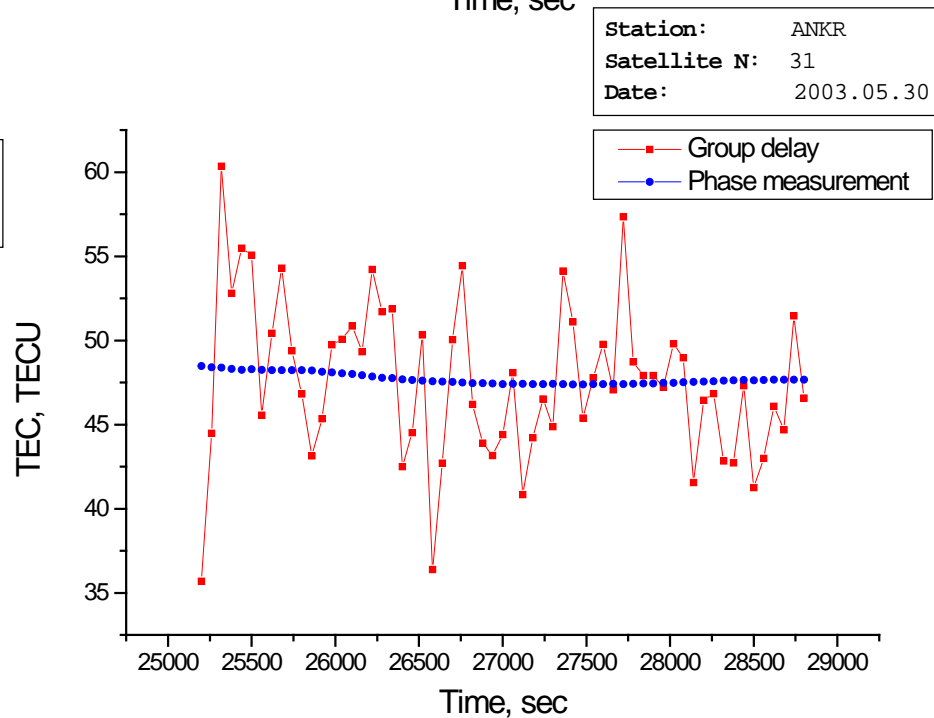
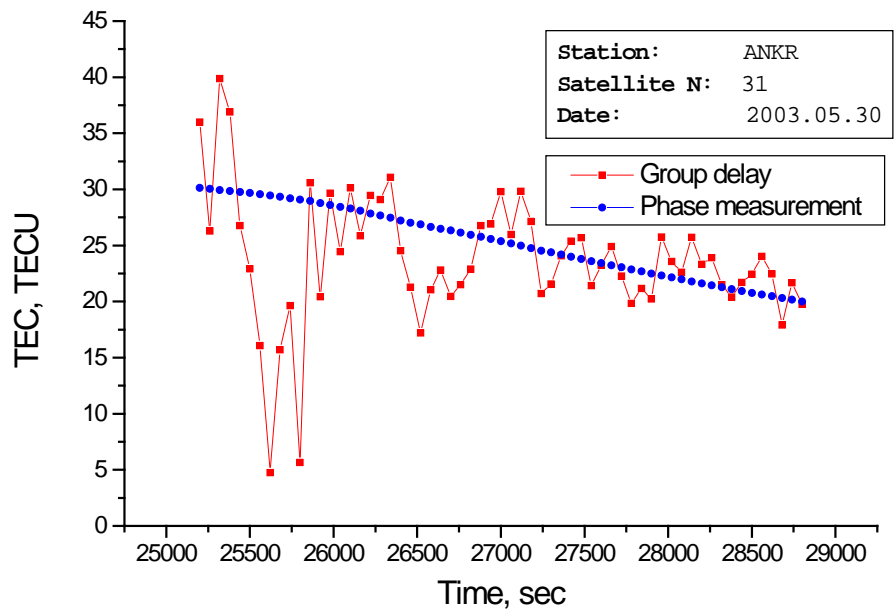
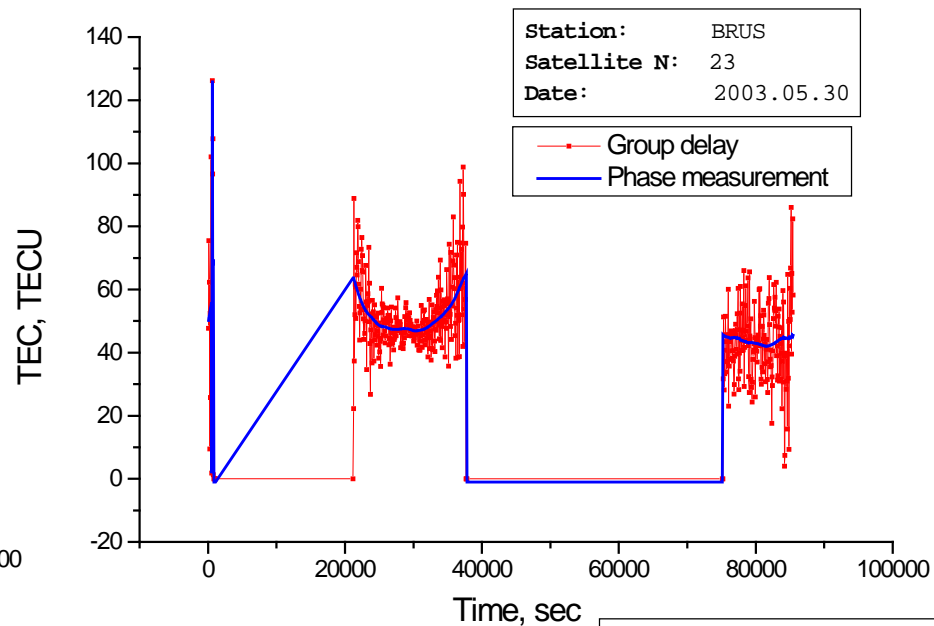
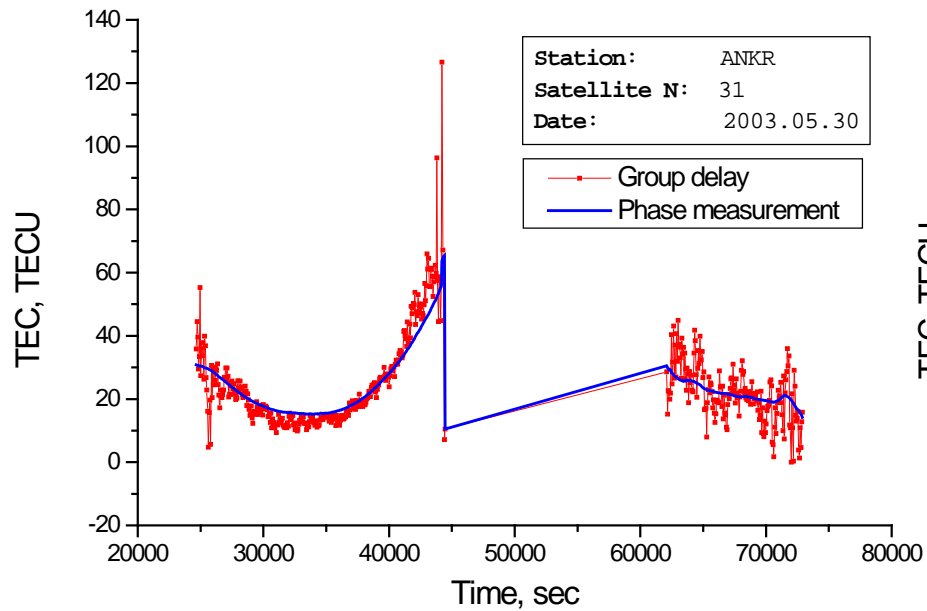
$$\text{LN} = \Phi + \xi + E, \quad E = \text{LN} - \text{PN}$$

$$\text{LN} = \Phi + \xi$$

$$\left. \begin{array}{l} \text{LN} = \Phi \\ \text{L}'\text{N}' = \Phi' \end{array} \right\} \rightarrow \text{AN} = \Phi - \Phi' = D$$

20-40km – vertical resolution

10-30km – horizontal resolution



Solution with Smoothing

$$Af = \Psi \quad \min \|f - f_0\|_{W_n}^2$$

SIRT:

$$\vec{x}^{k+1} = \vec{x}^k + \sum_i \rho_i \frac{y_i - (\vec{a}_i, \vec{x}^k)}{(\vec{a}_i, \vec{a}_i)} \vec{a}_i$$

$$\min \|\vec{x} - \vec{x}_0\|^2$$
$$A\vec{x} = \vec{y}$$

Modified SIRT:

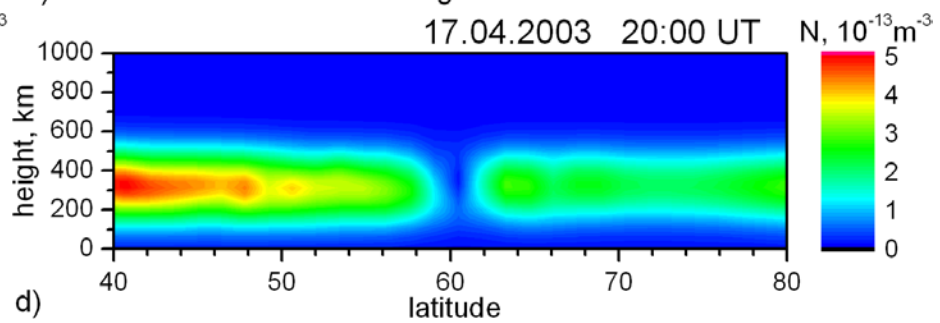
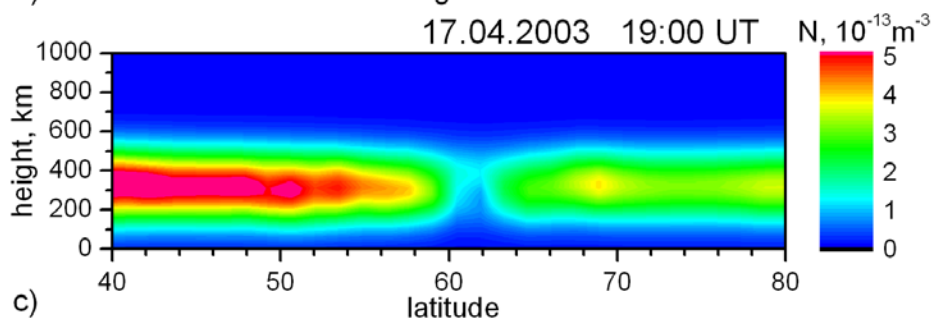
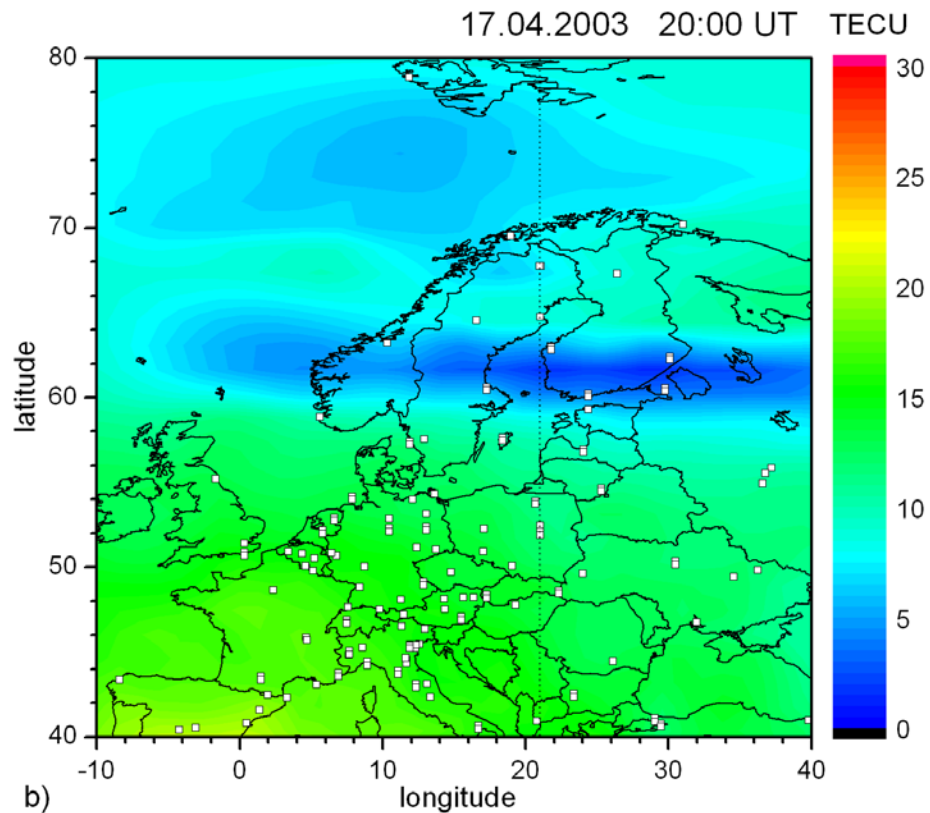
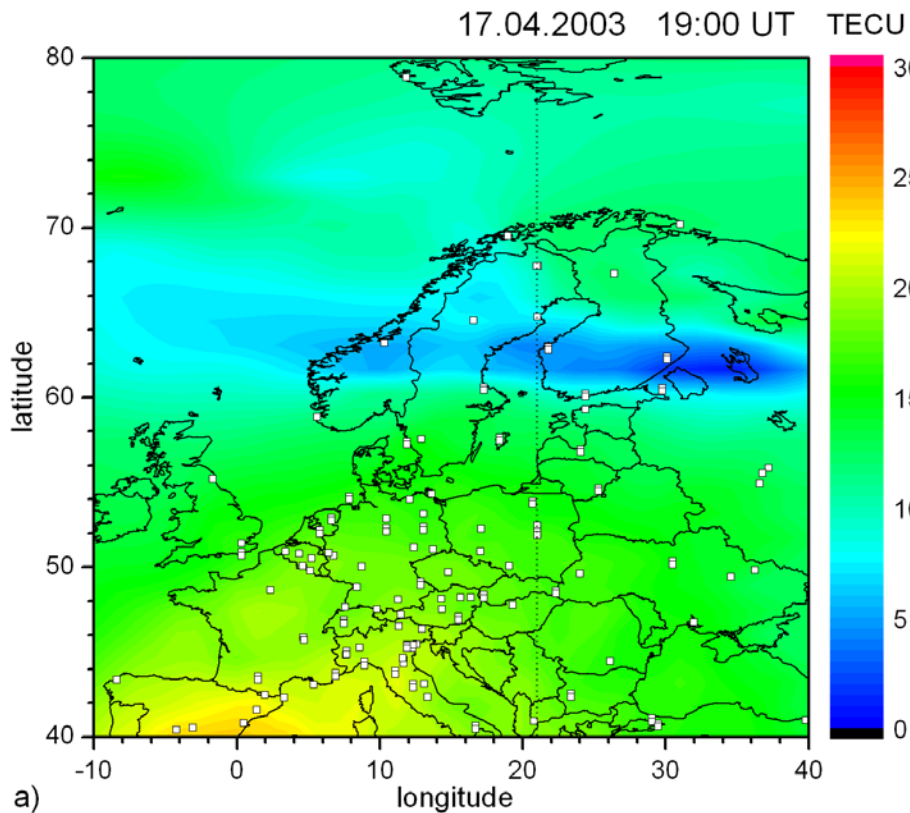
$$\vec{x}^{k+1} = \vec{x}^k + \sum_i \rho_i \frac{y_i - (\vec{a}'_i, \vec{x}^k)_L}{(\vec{a}'_i, \vec{a}'_i)_L} \vec{a}'_i$$

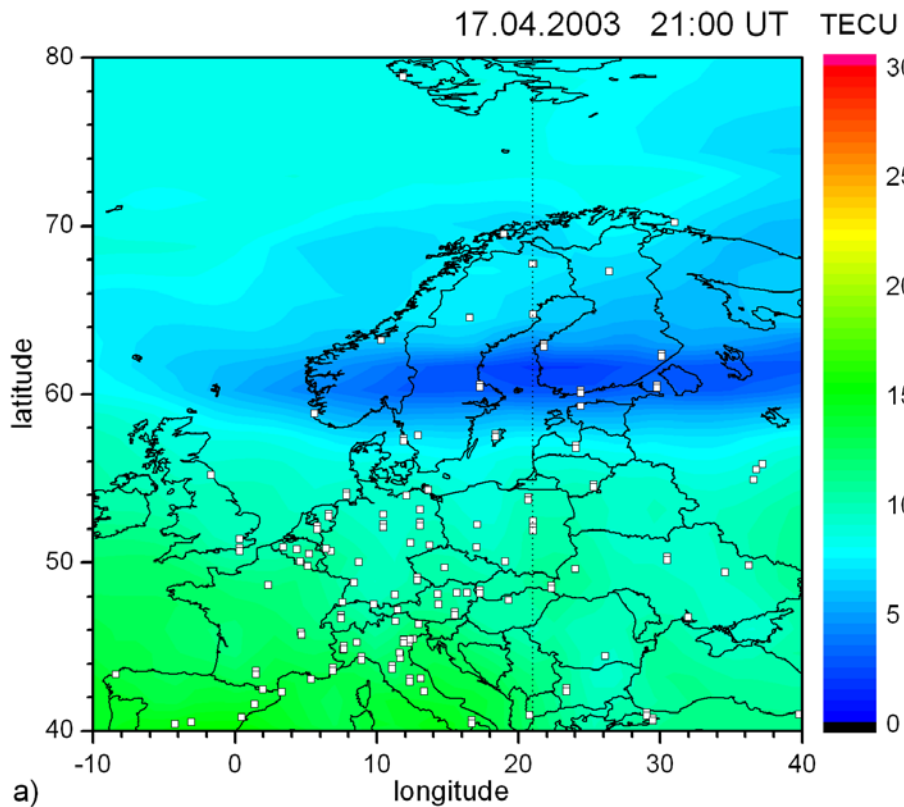
$$\min (\vec{x} - \vec{x}_0, \vec{x} - \vec{x}_0)_L$$
$$A\vec{x} = \vec{y}$$

$$\vec{a}'_i = (L^*L)^{-1} \vec{a}_i$$

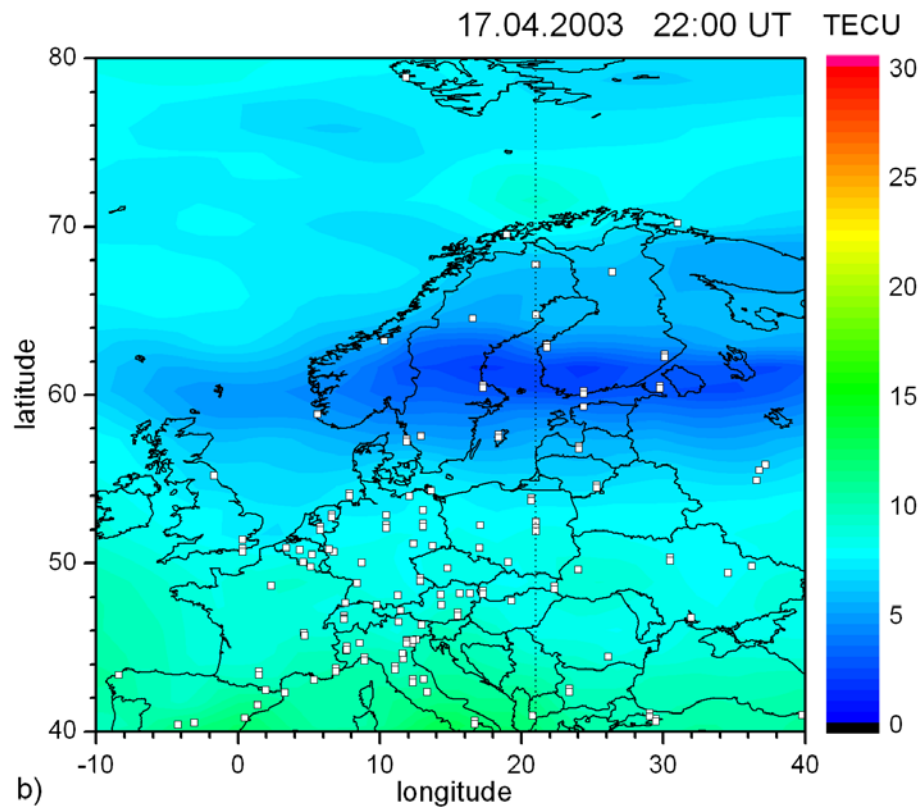
$$\vec{x}^{k+1} = \vec{x}^k + t (L^*L)^{-1} \sum_i \vec{a}_i (y_i - (\vec{a}_i, \vec{x}^k))$$

$$(\vec{z}, \vec{x})_L = (L\vec{z}, L\vec{x}) = (\vec{z}, L^*L\vec{x})$$

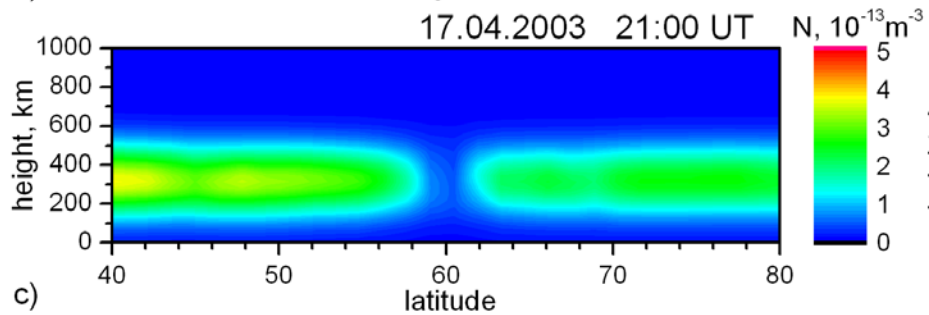




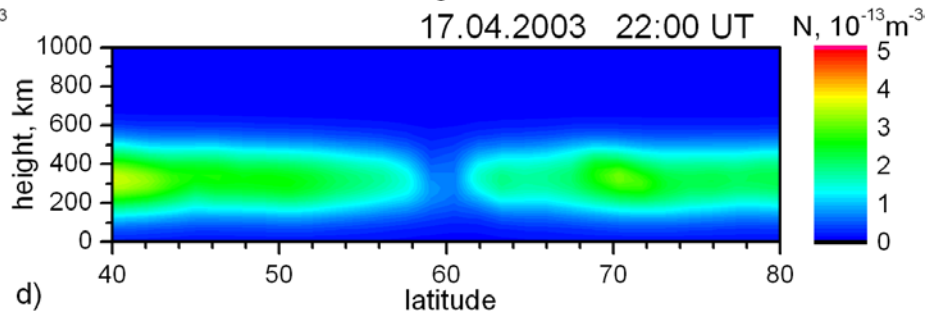
a)



b)

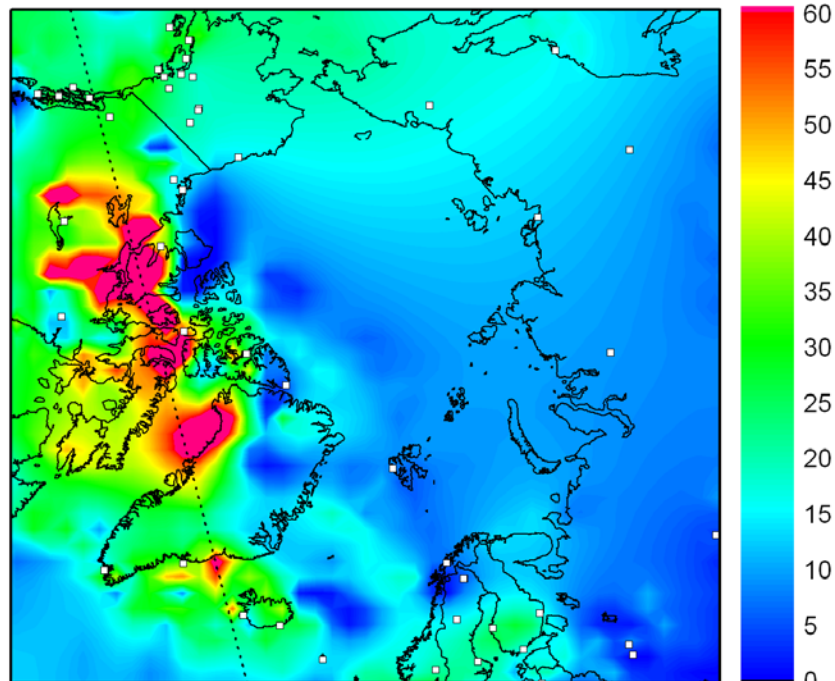


c)



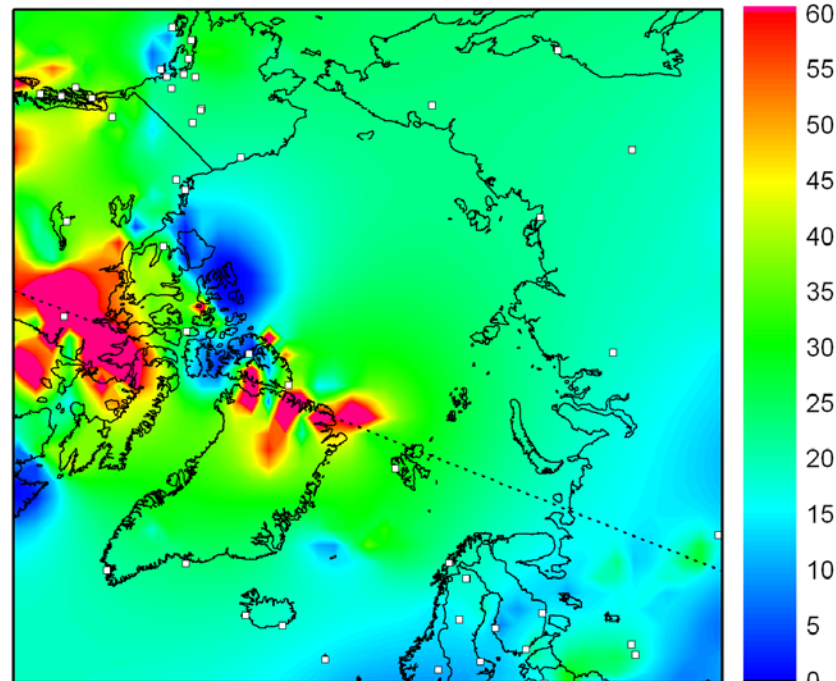
d)

29.10.2003 22:00 UT TECU



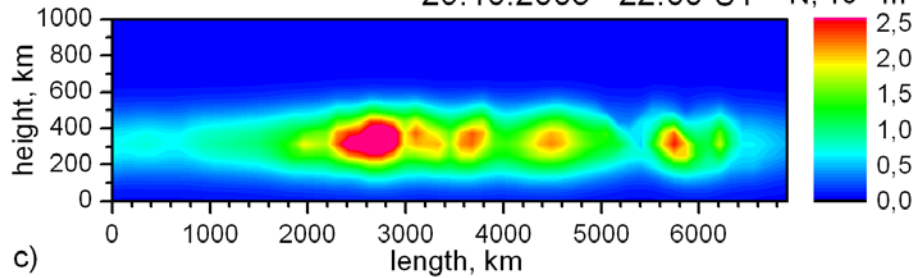
a)

30.10.2003 21:00 UT TECU



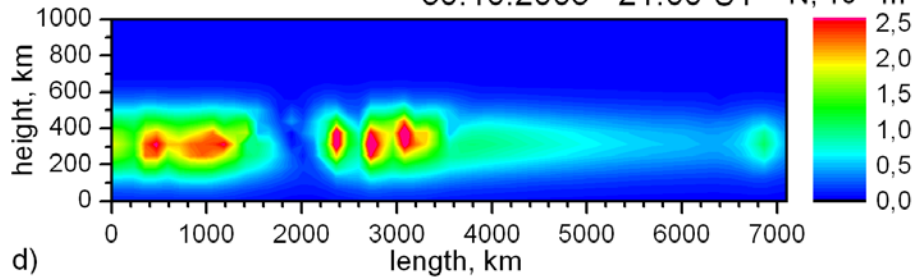
b)

29.10.2003 22:00 UT $N, 10^{-12} m^{-3}$



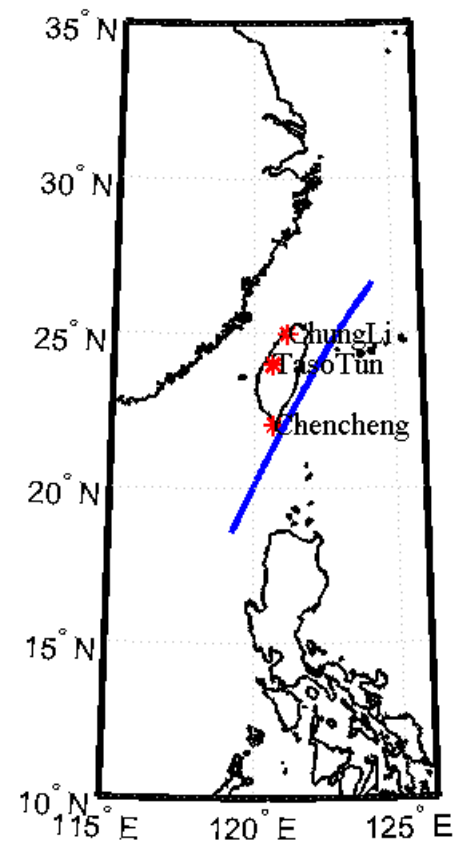
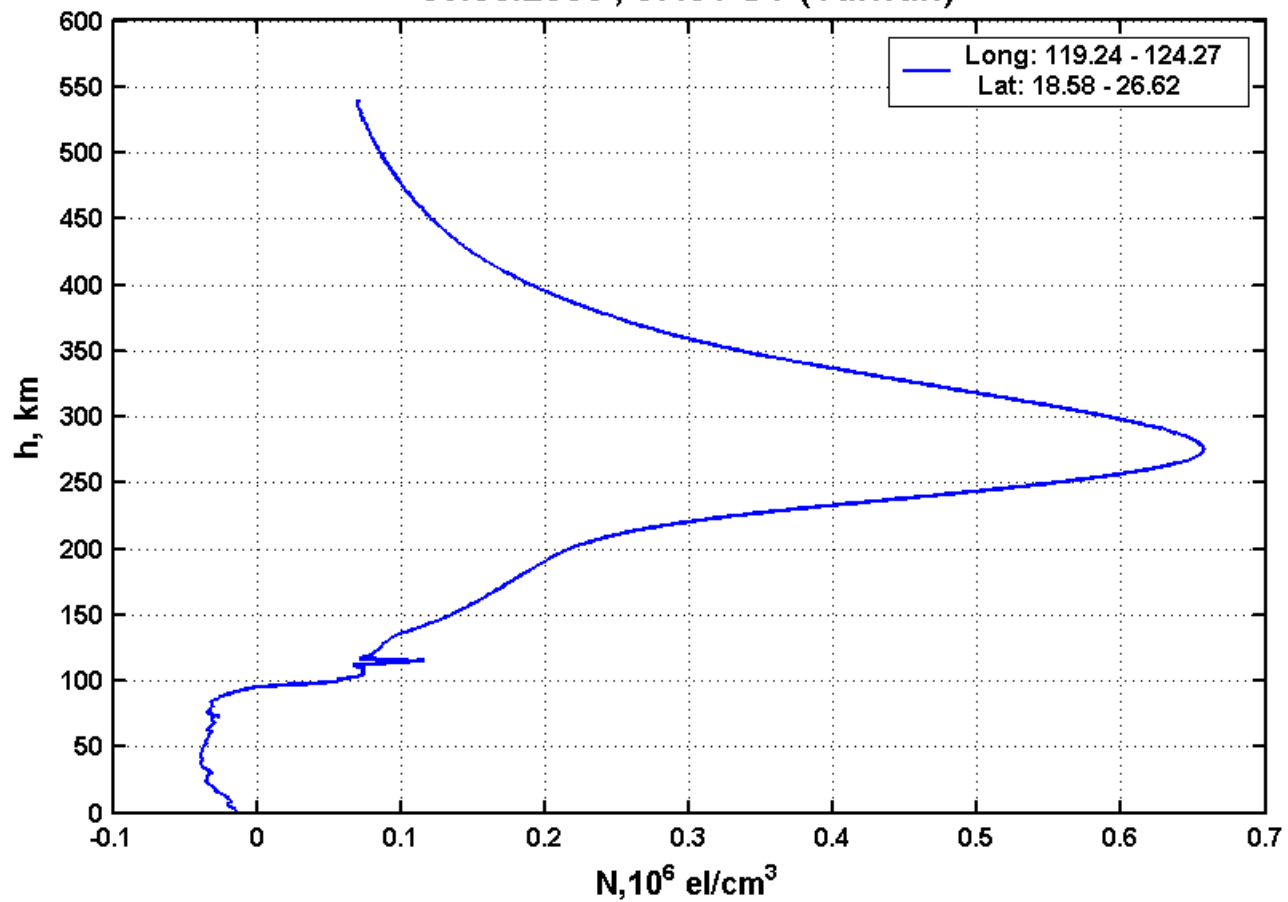
c)

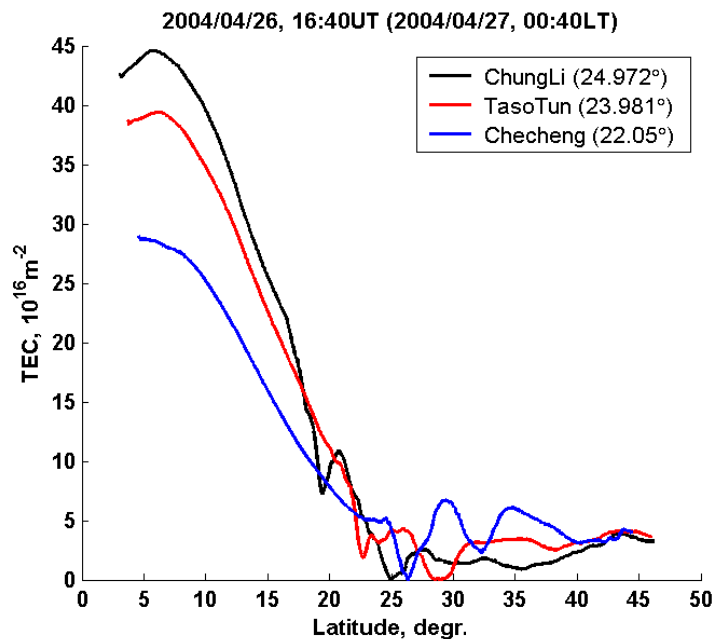
30.10.2003 21:00 UT $N, 10^{-12} m^{-3}$



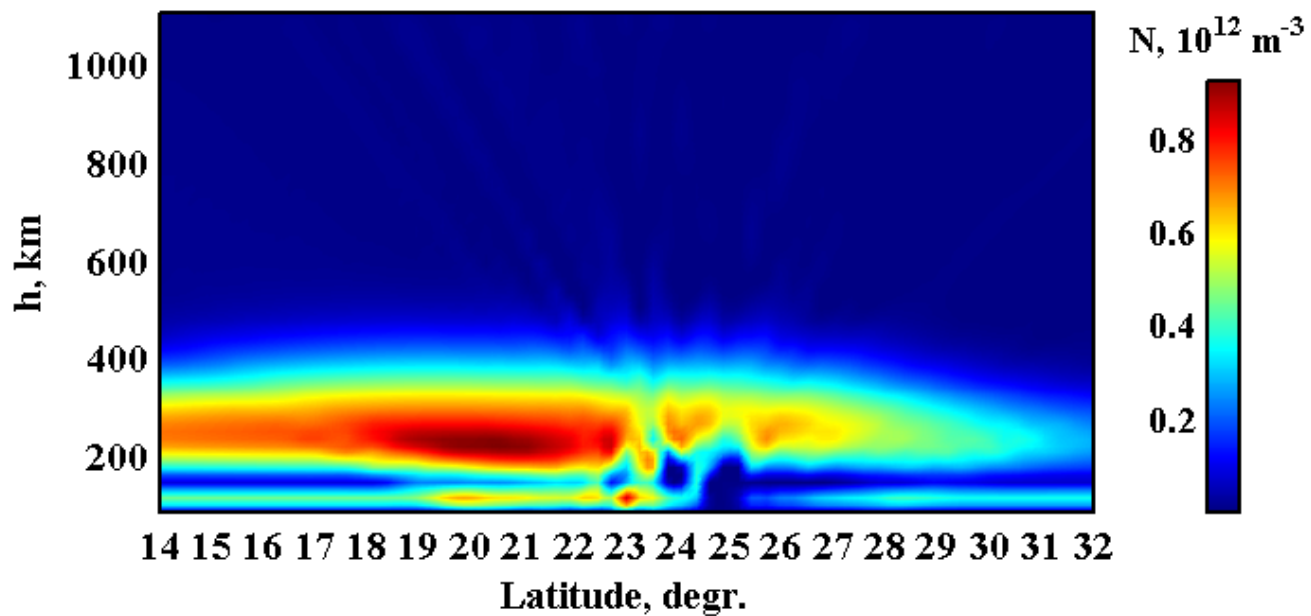
d)

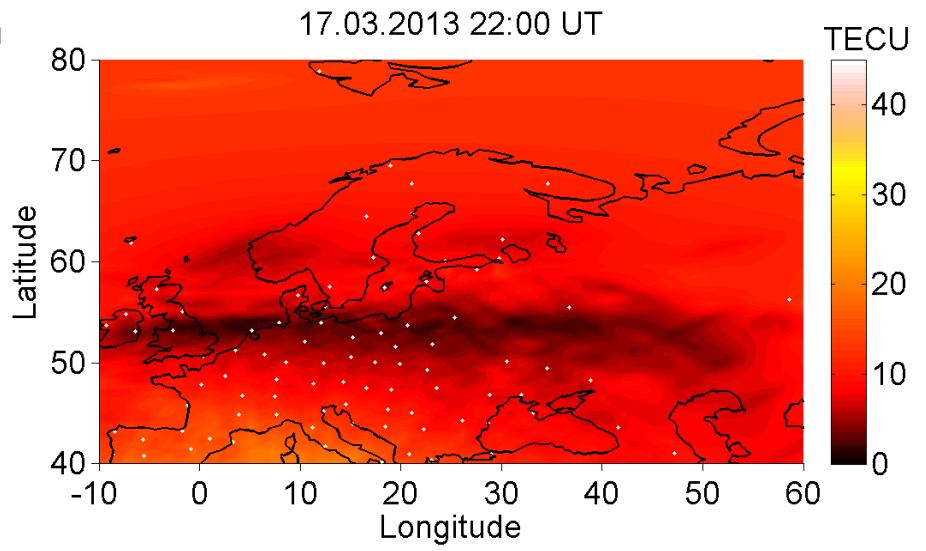
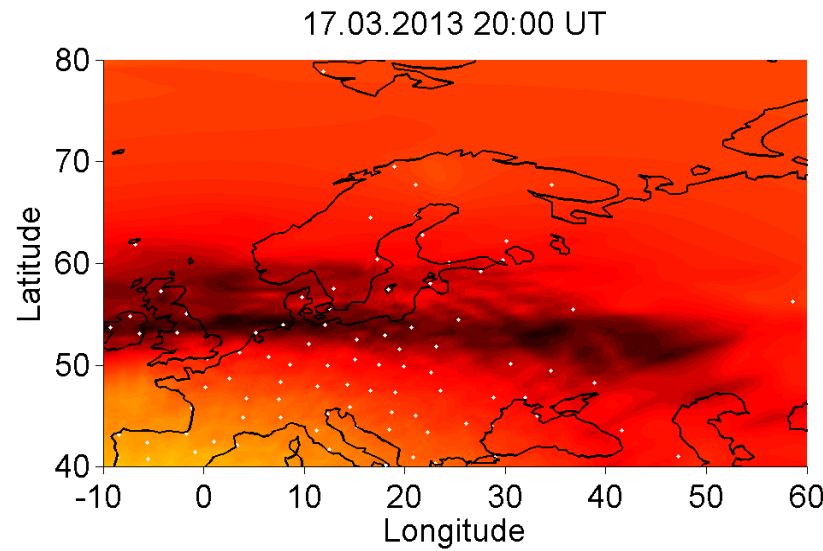
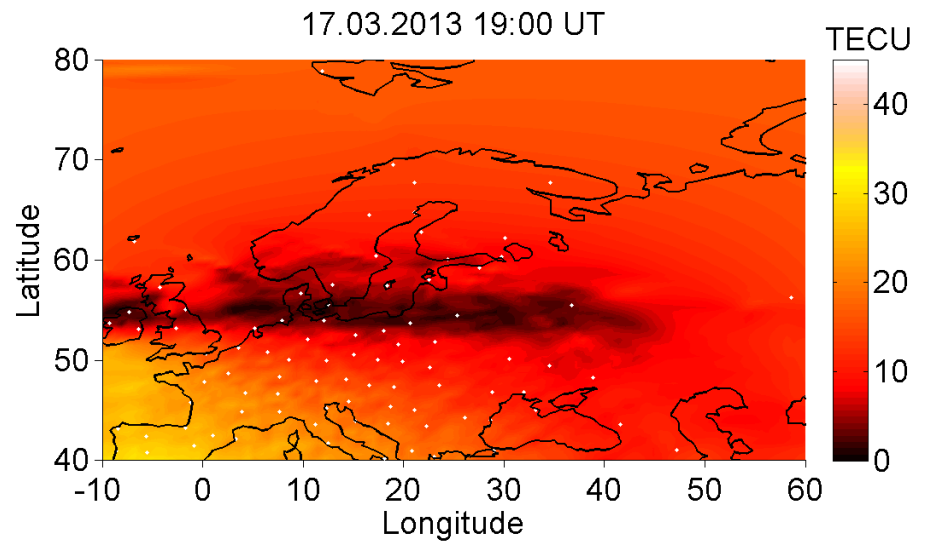
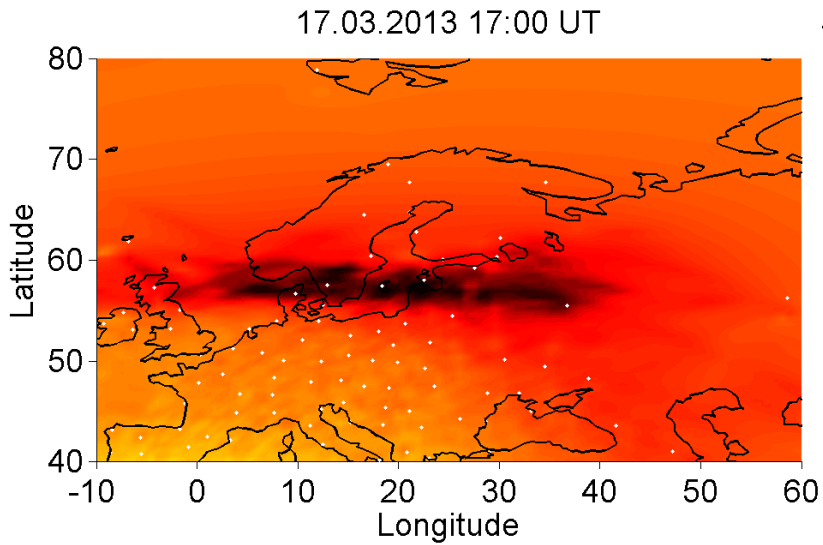
09.08.2006 , 07:51 UT (Taiwan)



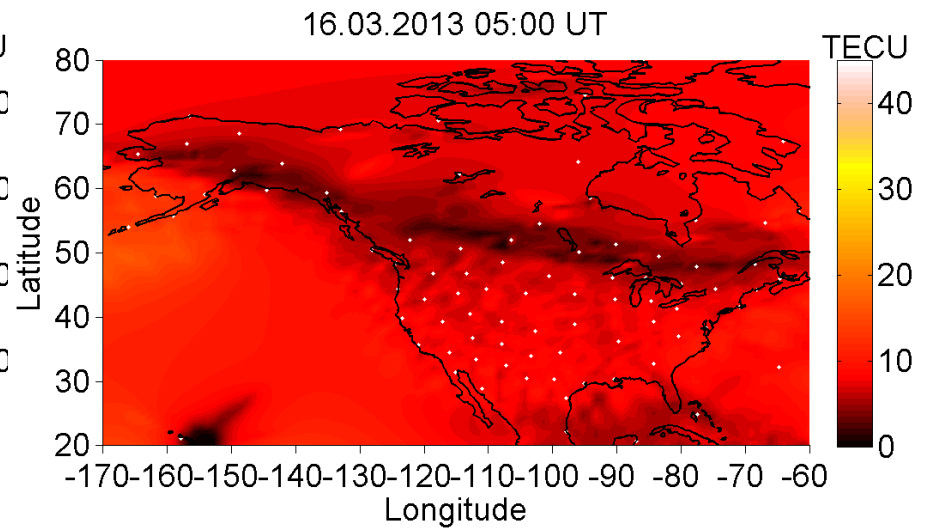
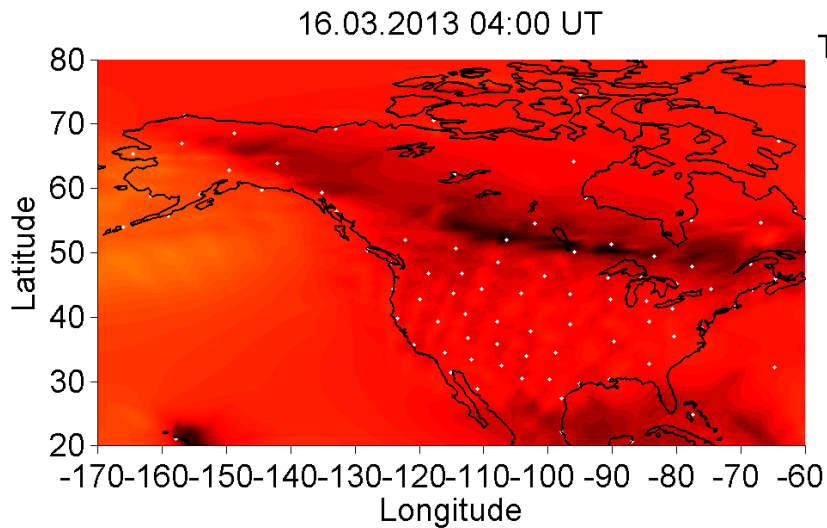
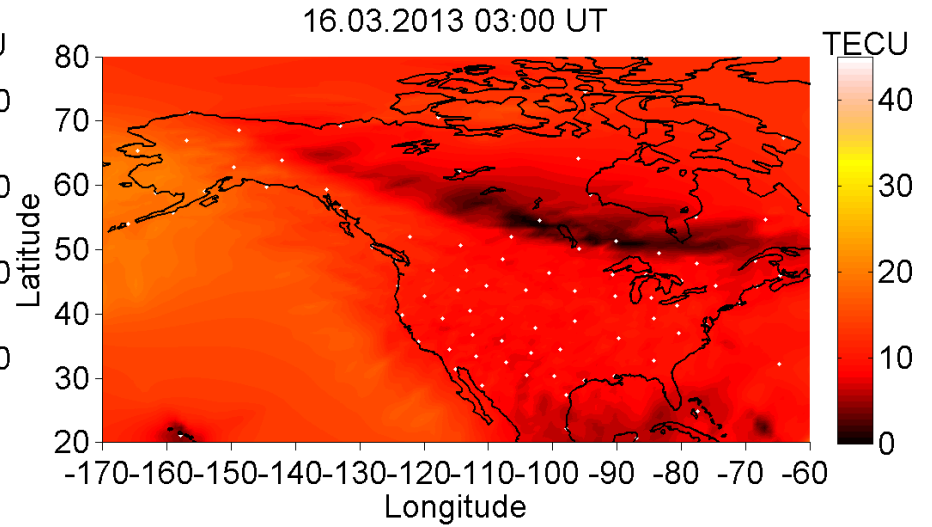
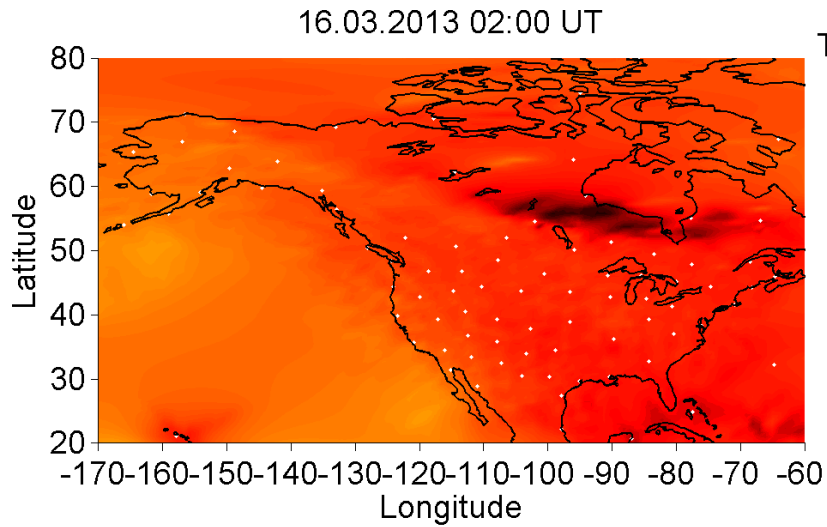


2006/04/26, 16:40UT

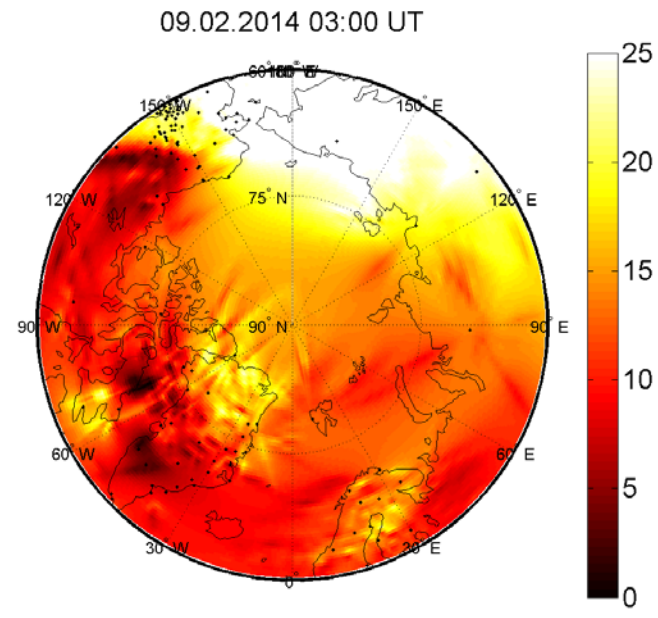
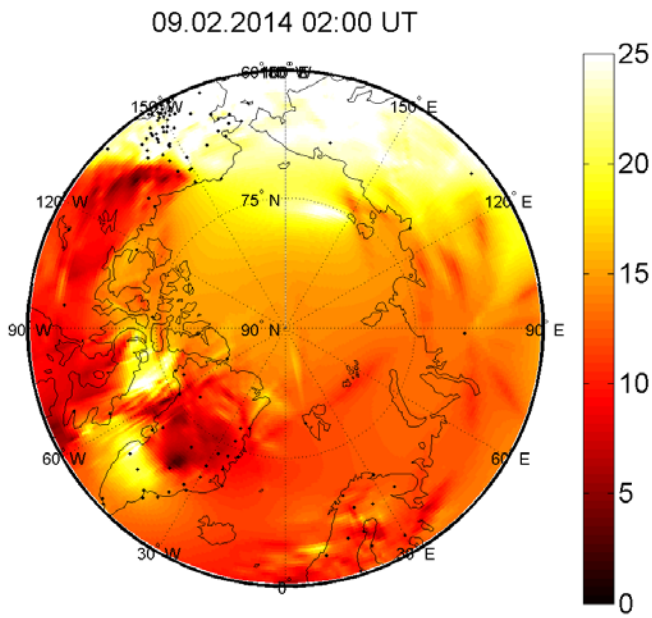




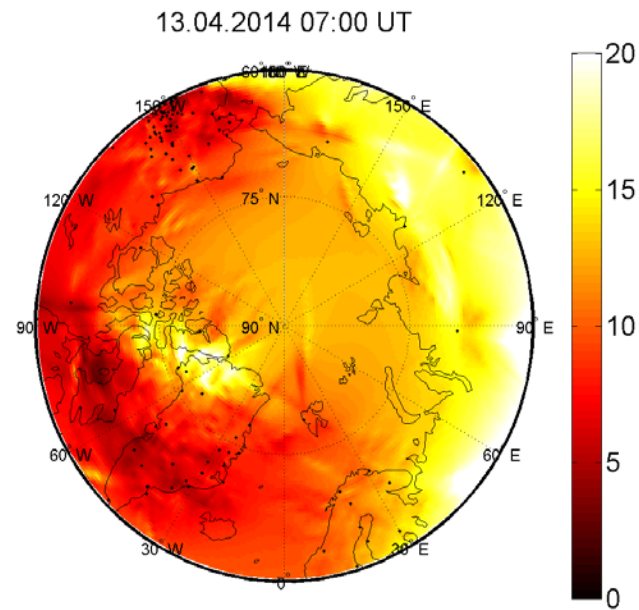
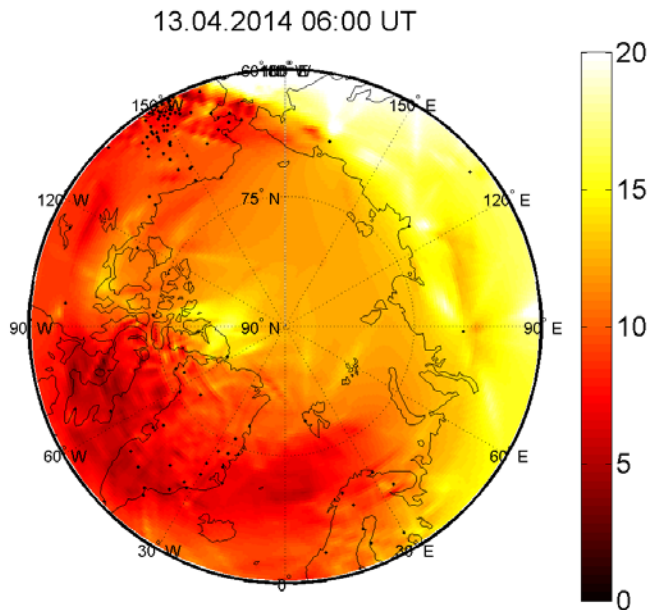
The example of evolution of the ionization trough above Europe on March 17, 2013, 17:00-22:00 UT (Kp=6.7)



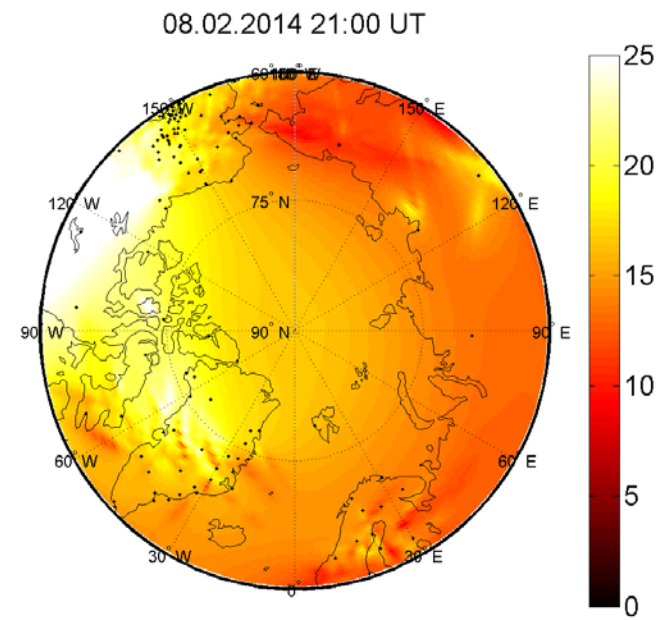
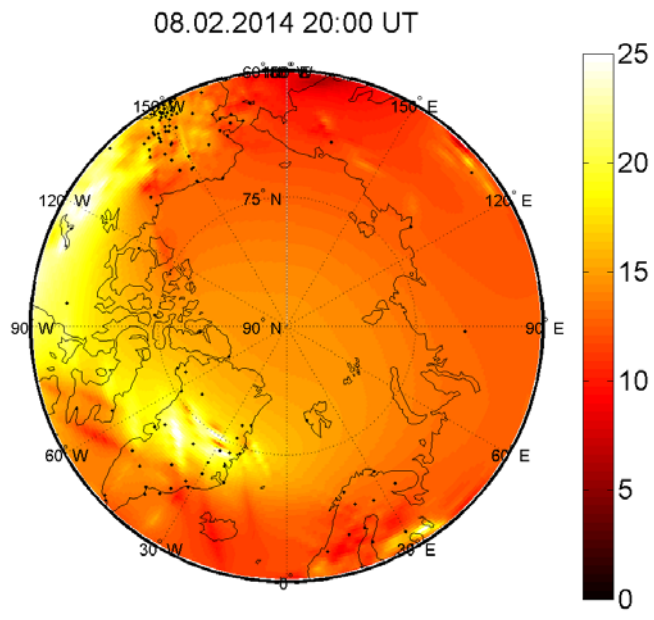
The example of evolution of the ionization trough above North America on March 16 , 2013, 02:00-05:00 UT ($K_p=3.3$)



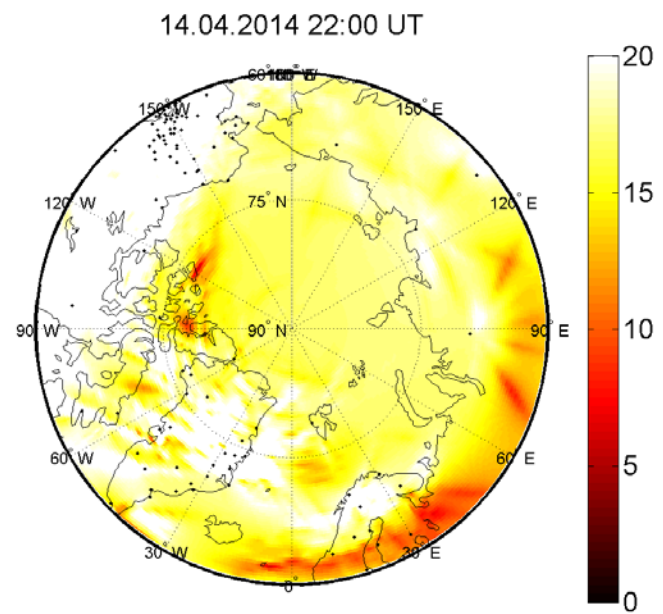
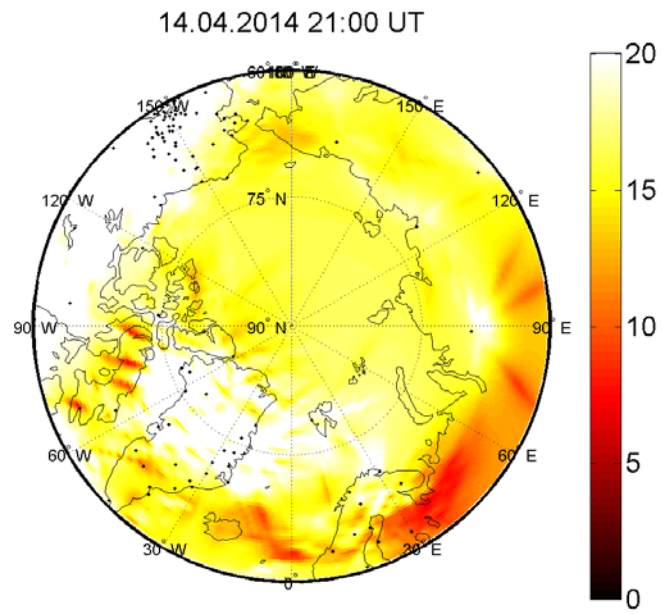
TEC maps above the Arctic region on February 9, 2014 (02:00 and 03:00 UT)



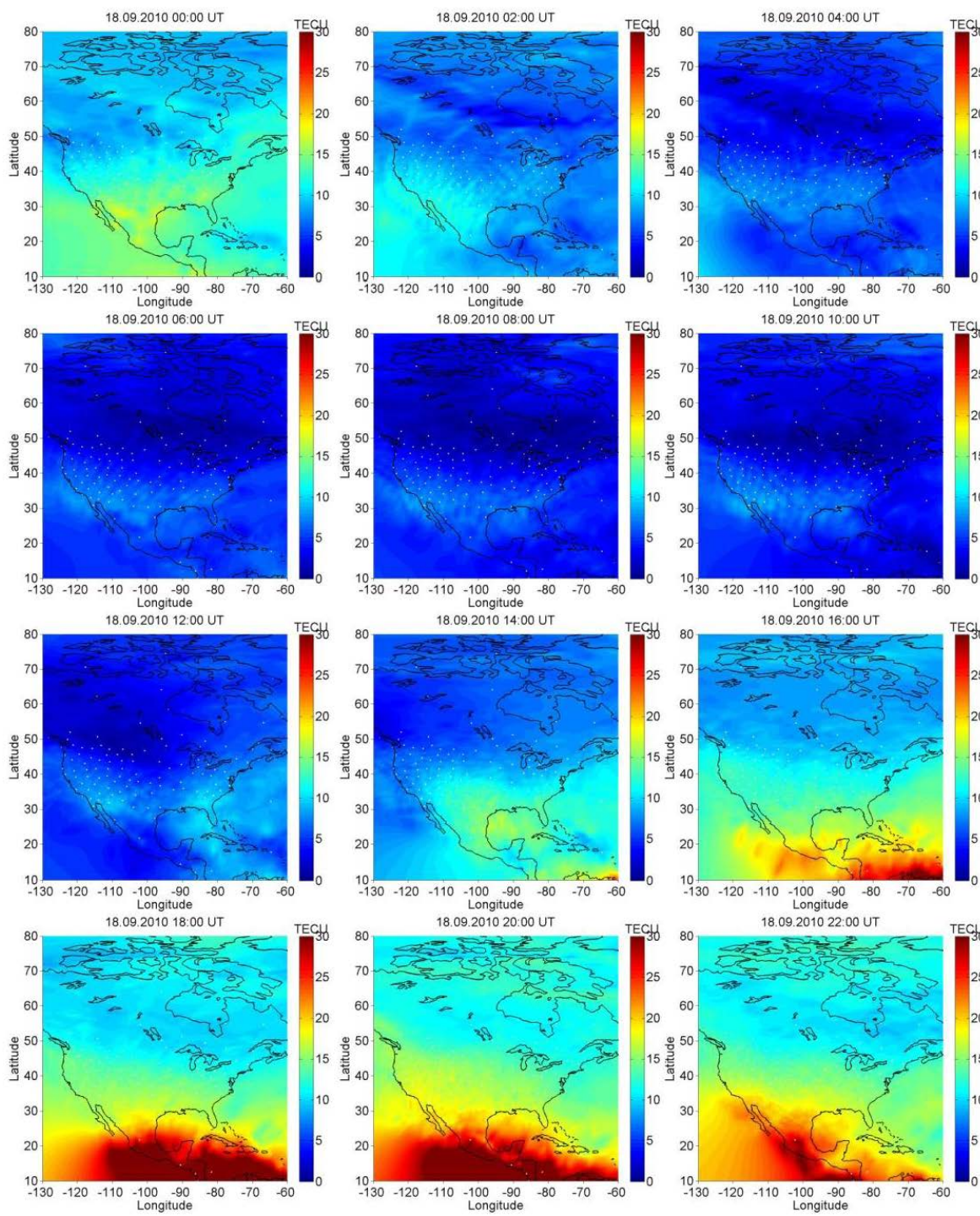
TEC maps above the Arctic region on April 13, 2014 (06:00 and 07:00 UT)



TEC maps above the Arctic region on February 8, 2014 (20:00 and 21:00 UT)



TEC maps above the Arctic region on April 14, 2014 (21:00 and 22:00 UT)

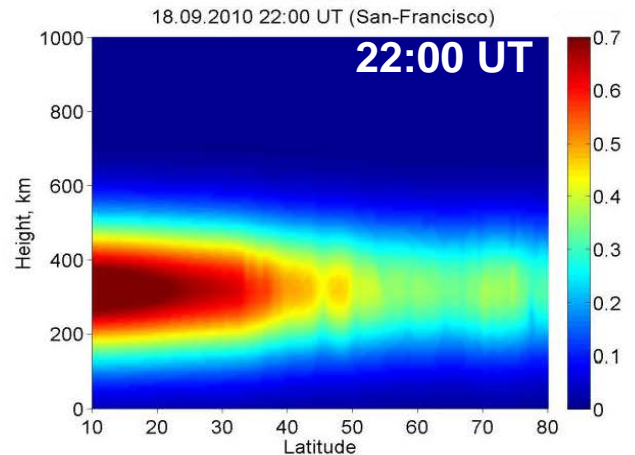
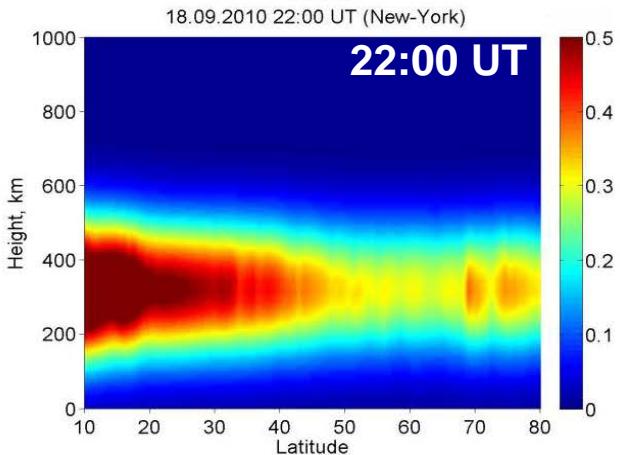
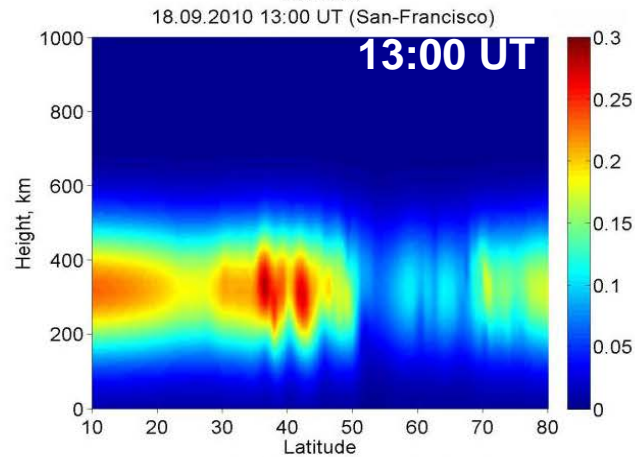
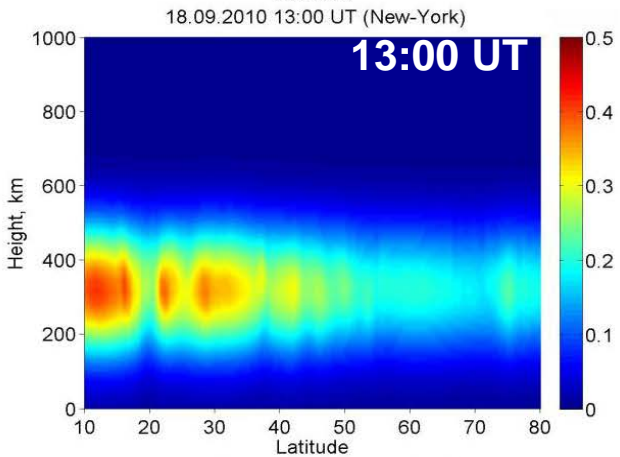
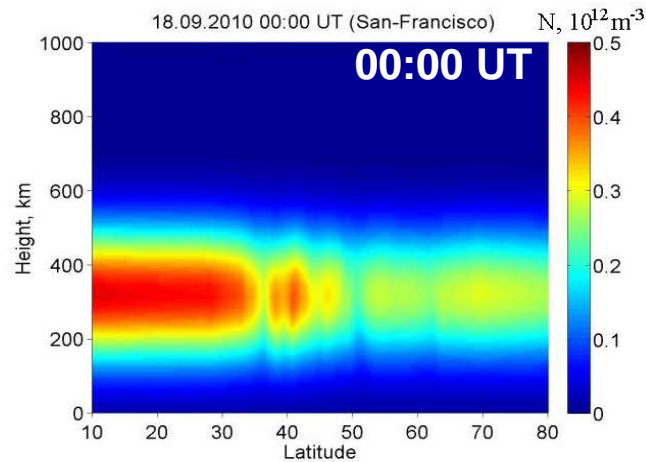
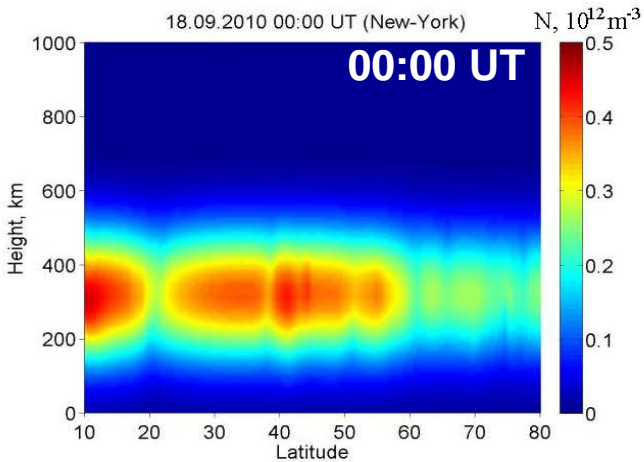


**Vertical TEC above
North America
according to
4D HORT during
18.09.2010
(00:00 UT-22:00 UT)**

New-York

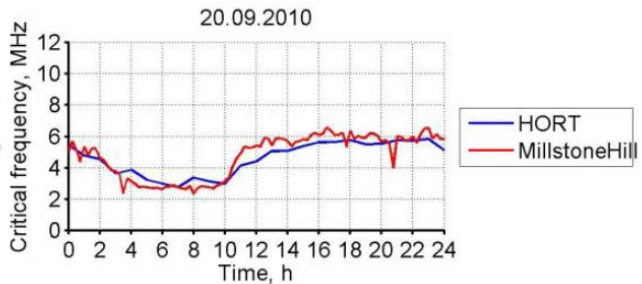
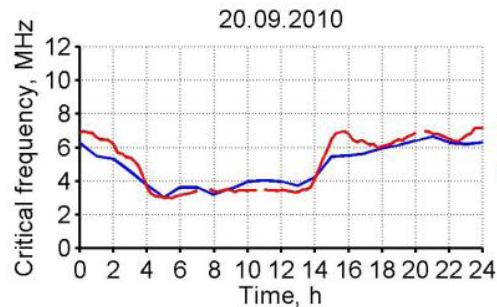
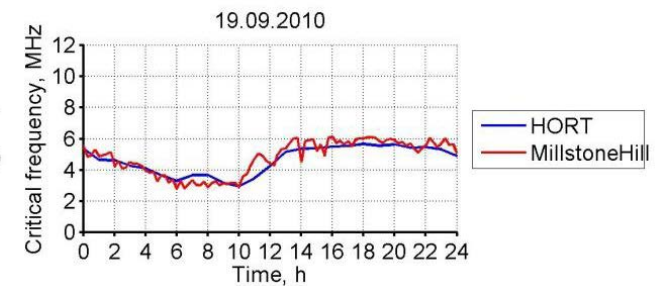
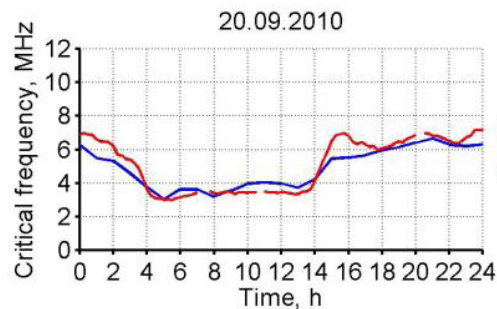
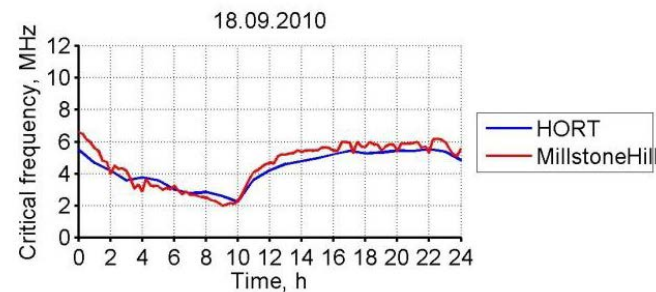
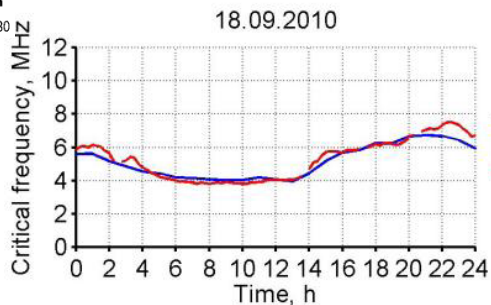
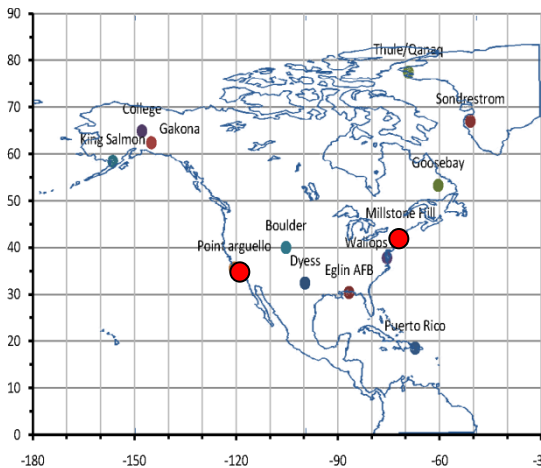
San-Francisco

Vertical cross-sections of the ionosphere along meridians of New-York and San-Francisco according to 4D HORT during 18.09.2010

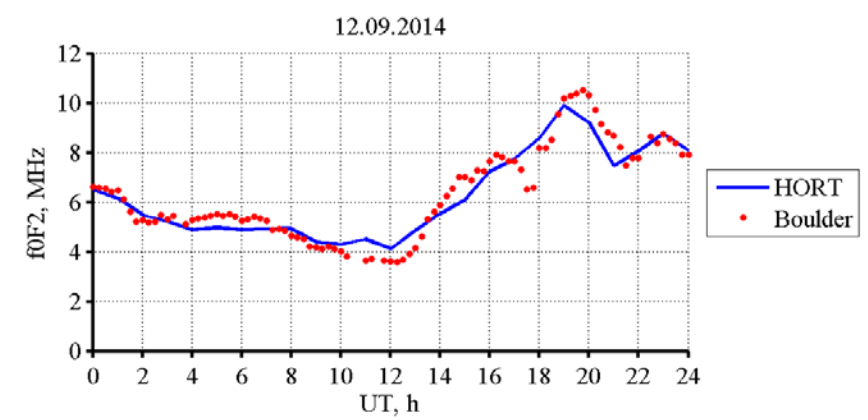
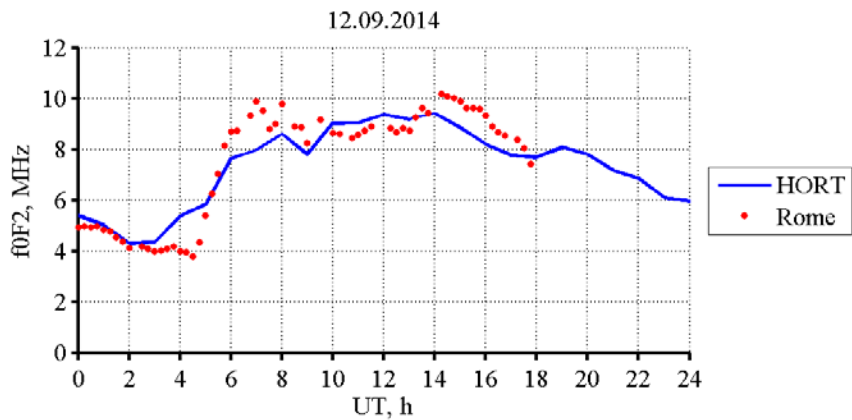
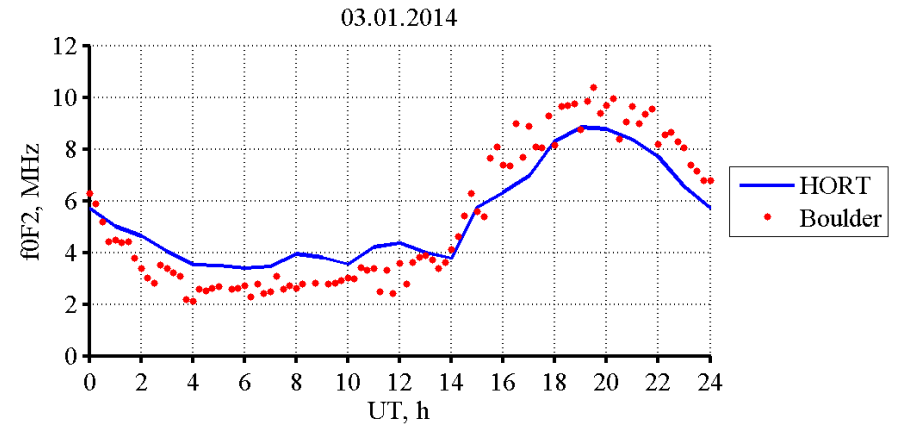
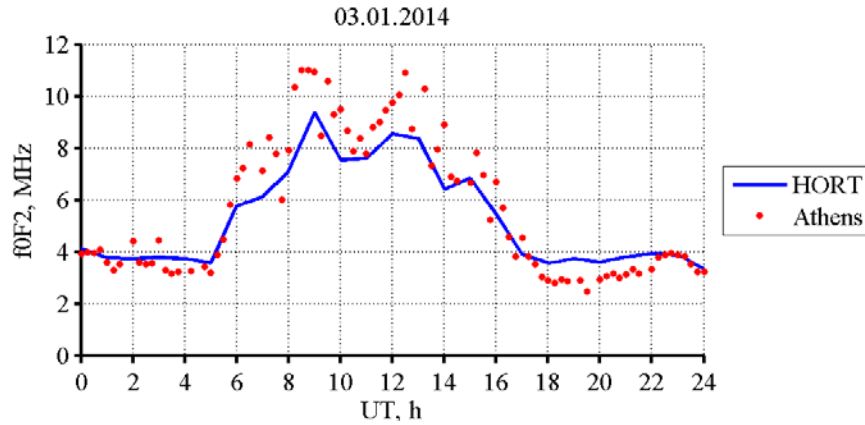


Comparison of HORT and ionosonde data

Sept. 18–20, 2010: f_oF2 as obtained from **HORT-images** and f_oF2 as obtained from **Point Arguello ionosonde & Millstone Hill ionosonde**.



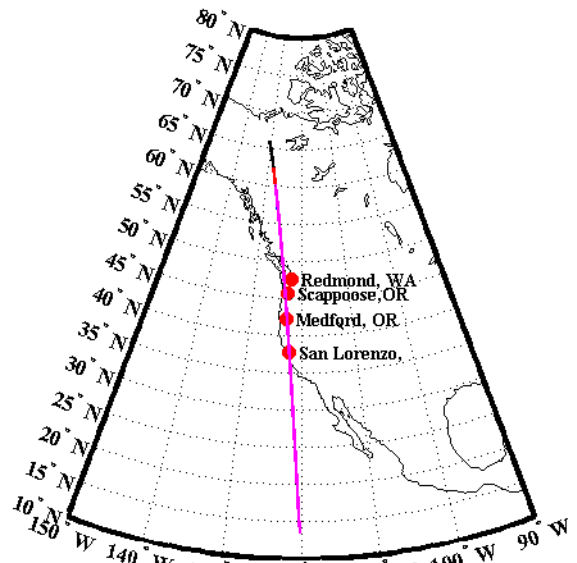
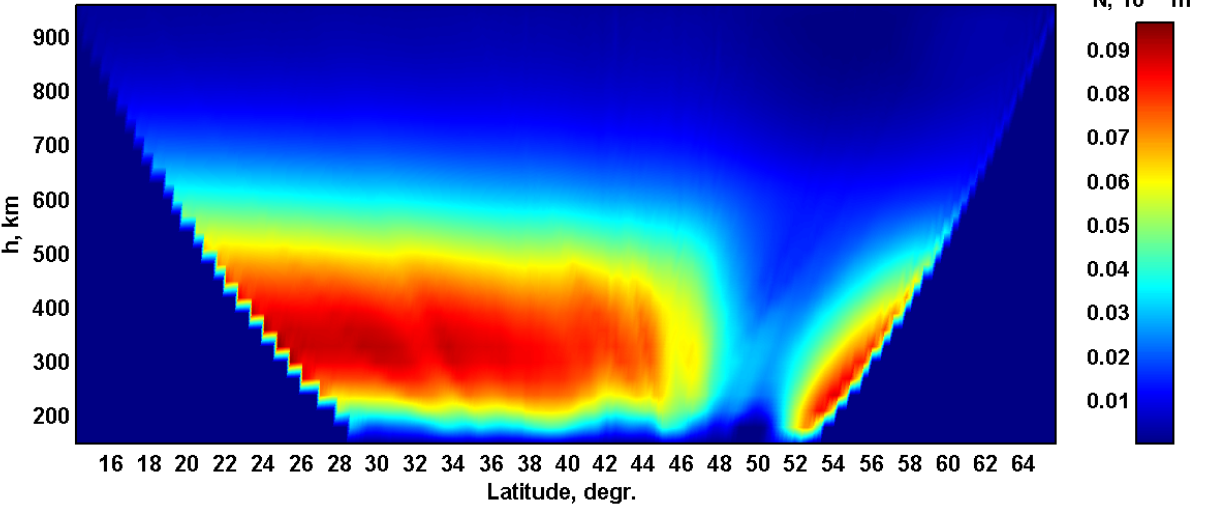
Comparison of HORT and ionosonde data



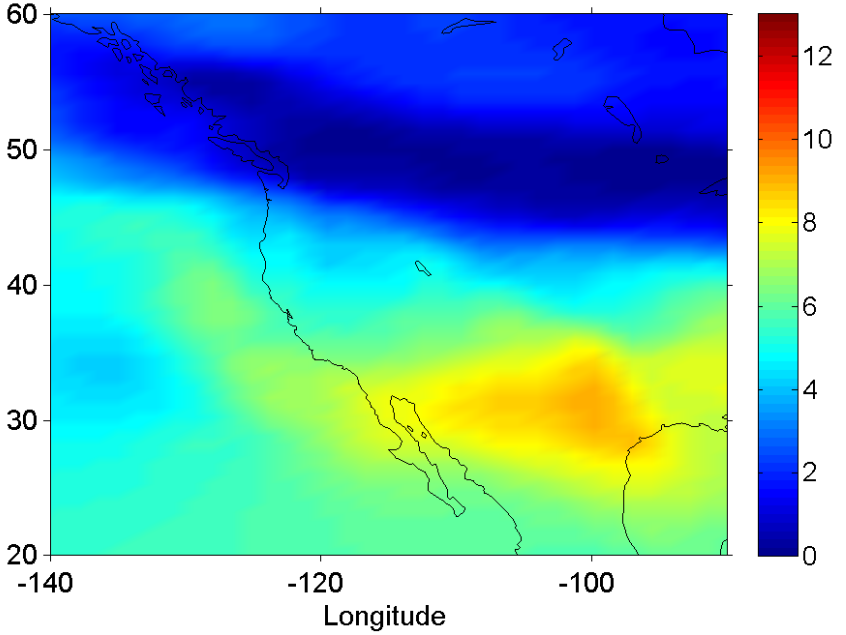
The analysis based on thousands of comparisons indicates that the diurnal behavior of f_0F_2 retrieved from HORT quite closely agrees with the ionosonde data. The discrepancies in critical frequencies are far below **0.5 MHz** during the geomagnetically quiet periods and above **1 MHz** during the disturbances.

U.S. West Coast

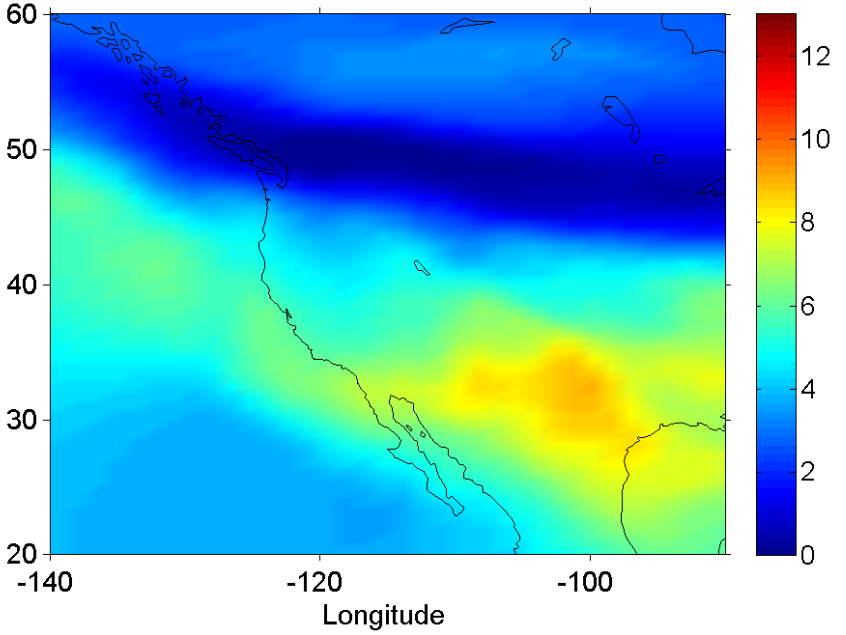
28.03.2013 , 10:36 UT (02:36 LT; -8h), COSMOS-2407



28.03.2013 10:00 UT TEC, TECU

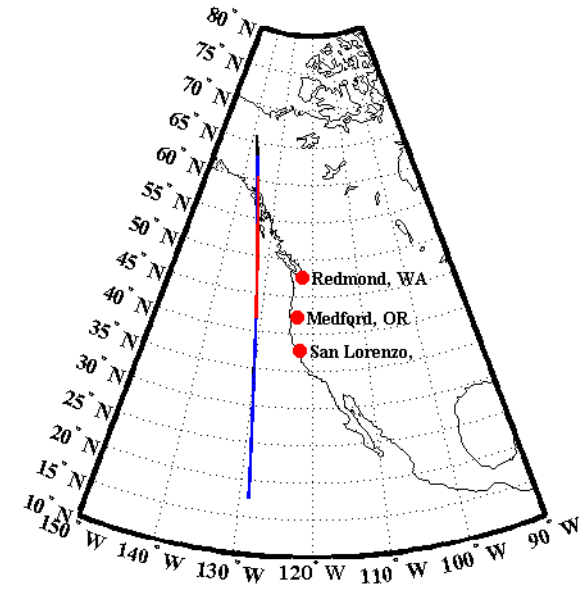
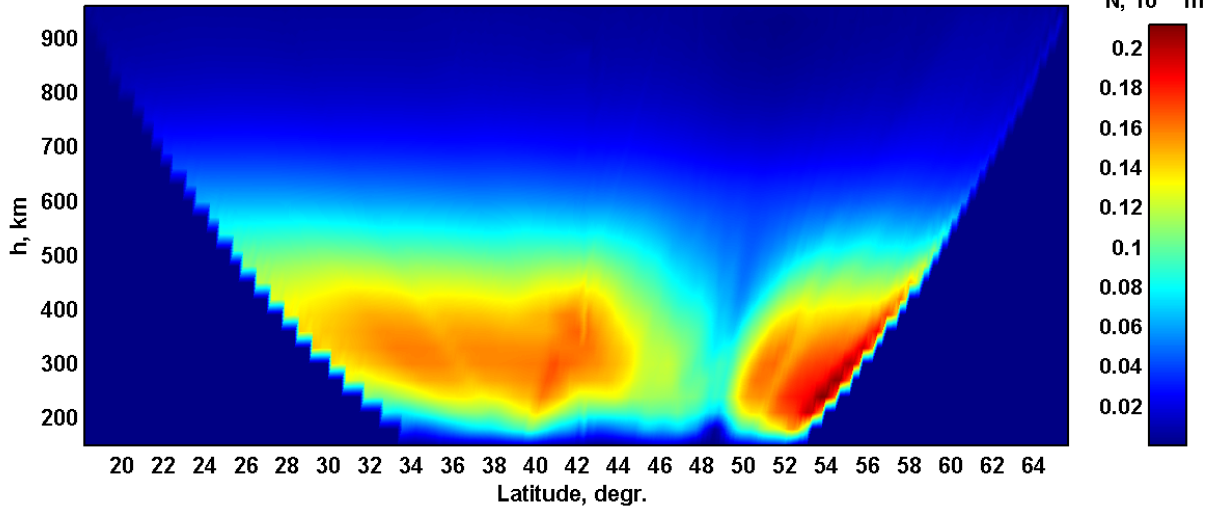


28.03.2013 11:00 UT TEC, TECU

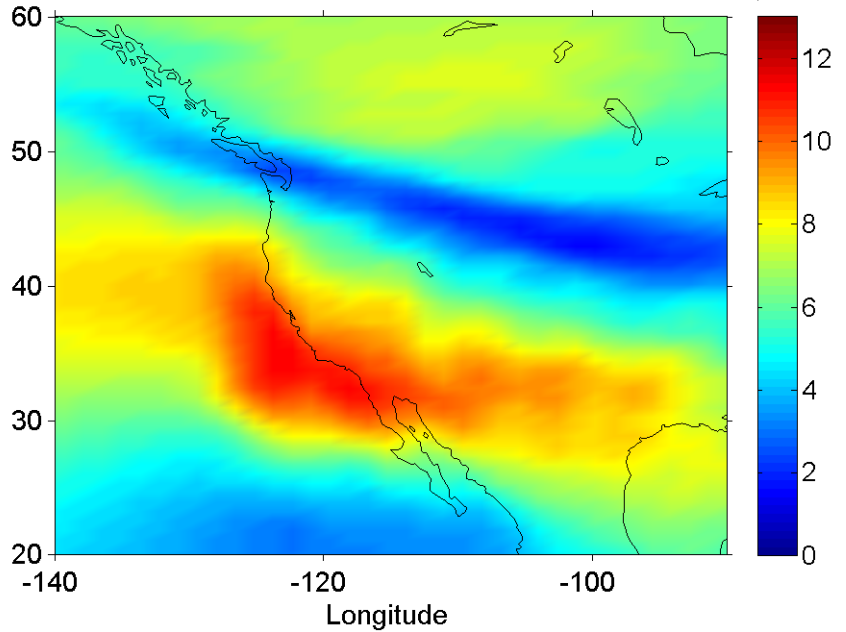


U.S. West Coast

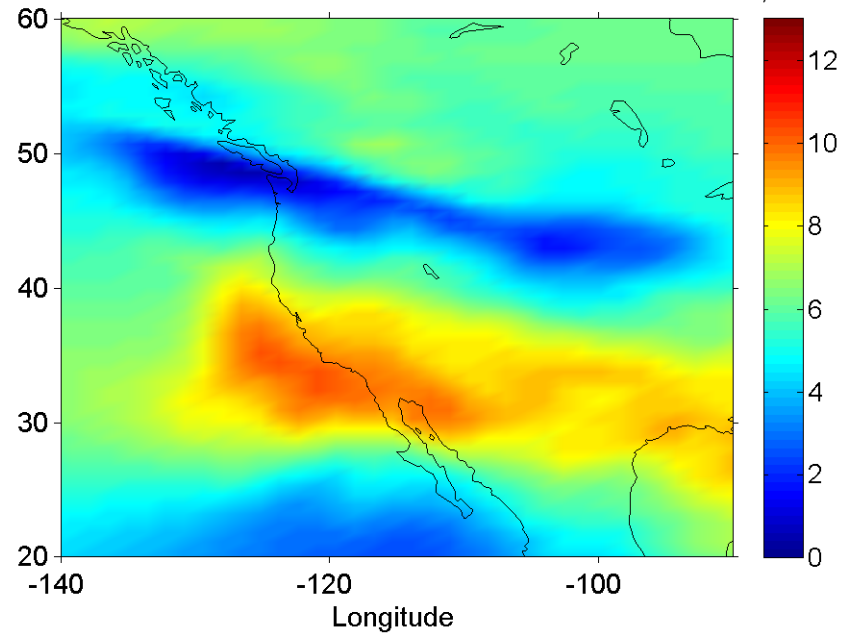
29.03.2013 , 11:03 UT (03:03 LT; -8h), COSMOS-2407



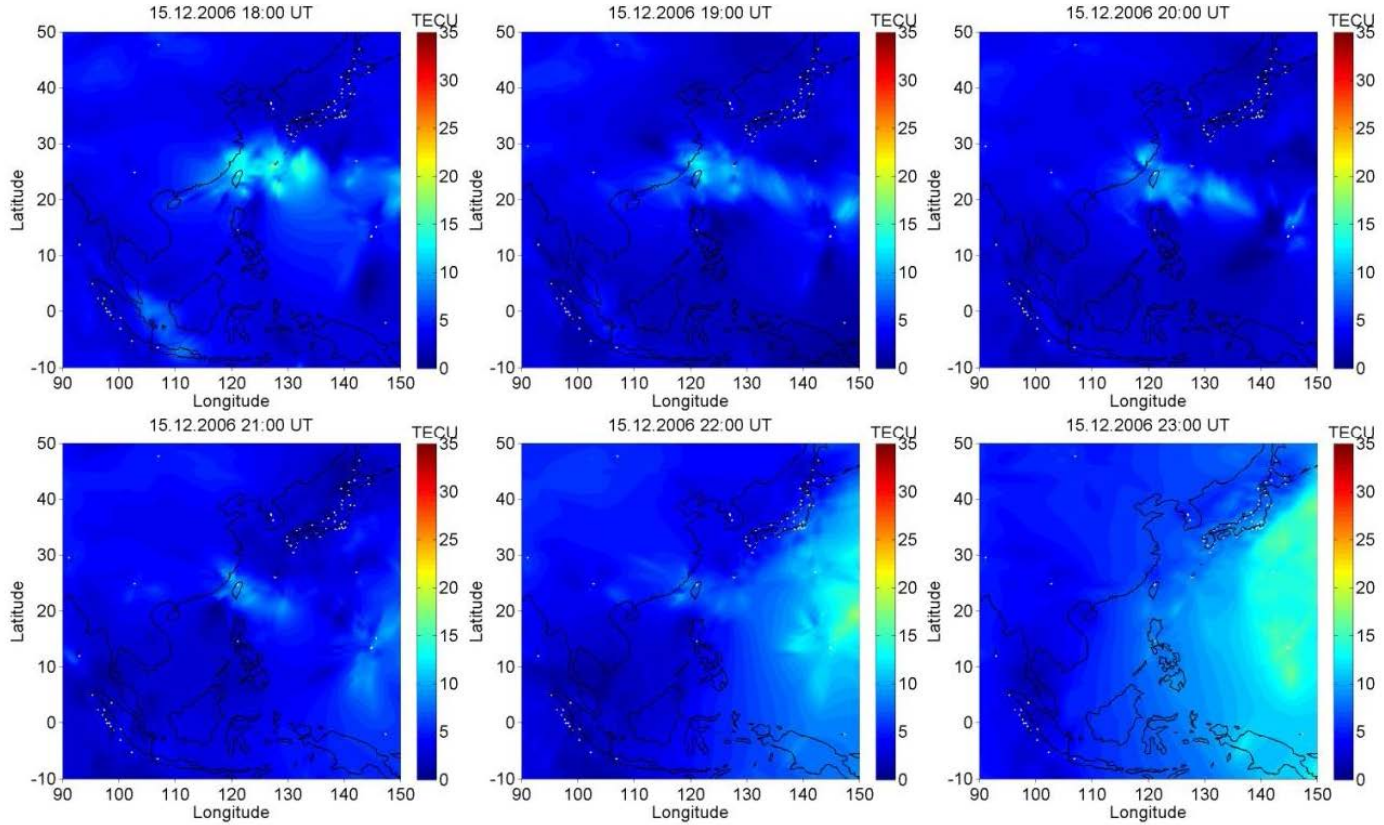
29.03.2013 11:00 UT TEC, TECU



29.03.2013 12:00 UT TEC, TECU

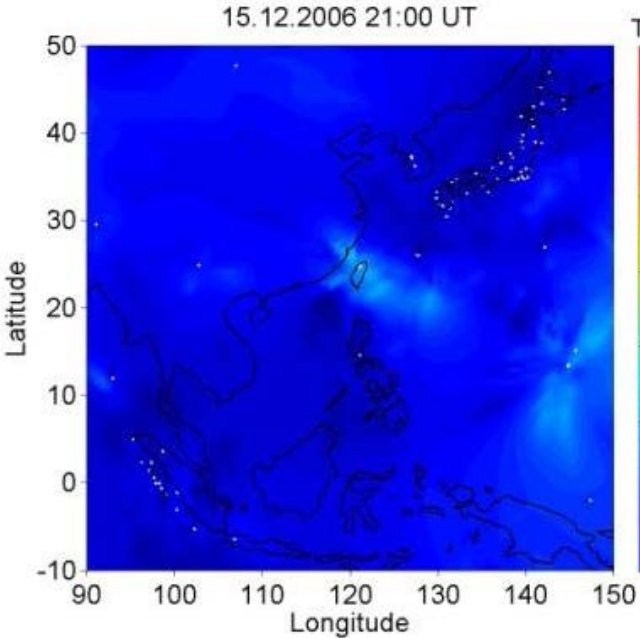


Vertical TEC above South-East Asia according to 4D HORT during geomagnetic storm 15.12.2006 (18:00 UT-23:00 UT)



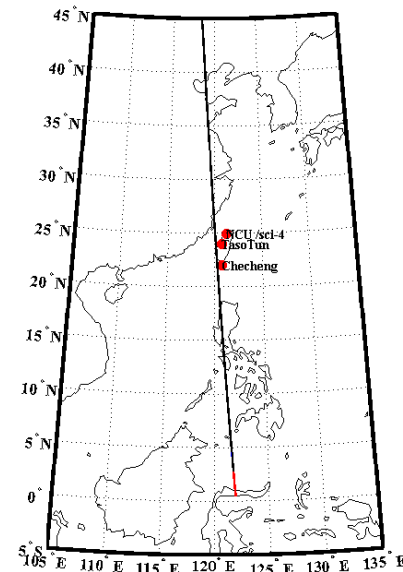
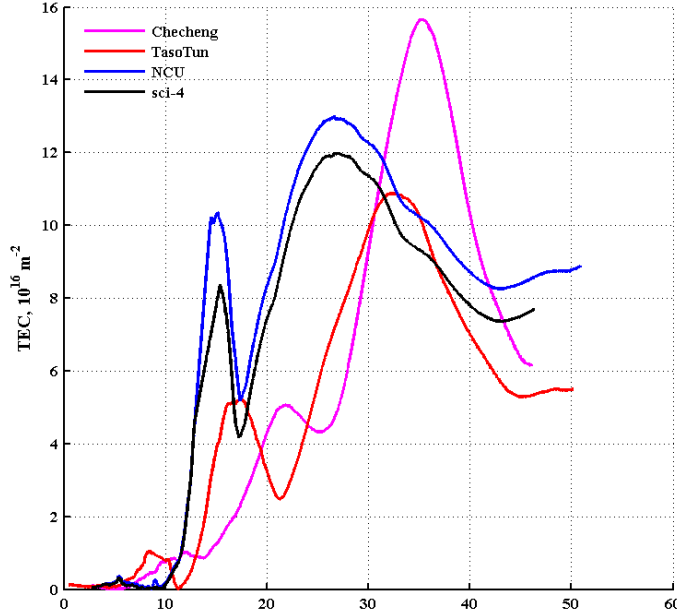
HORT

15.12.2006 21:00 UT

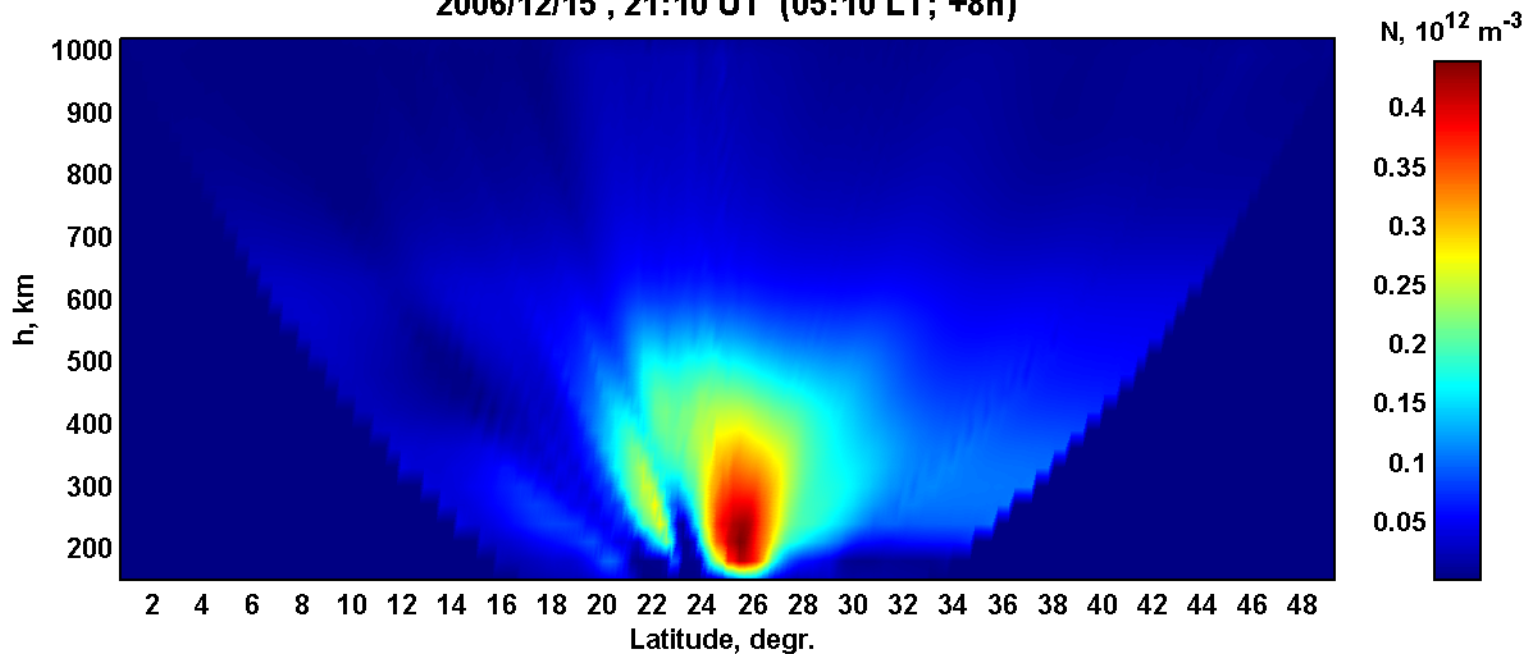


LORT

2006/12/15, 21:10 UT (05:10 LT; +8h), max(elev)= 86.33, OSCAR-32 (S->N)

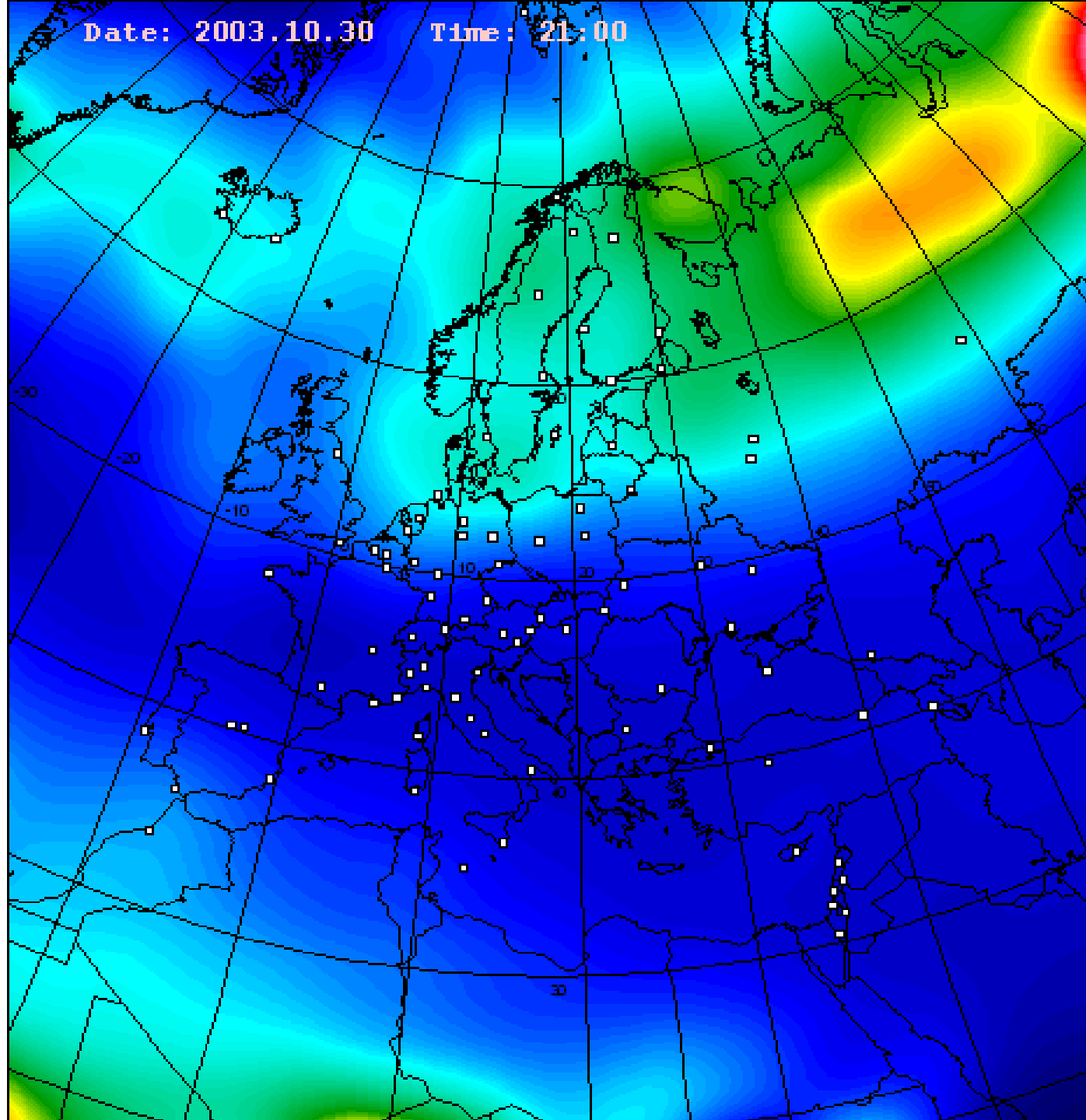


2006/12/15, 21:10 UT (05:10 LT; +8h)



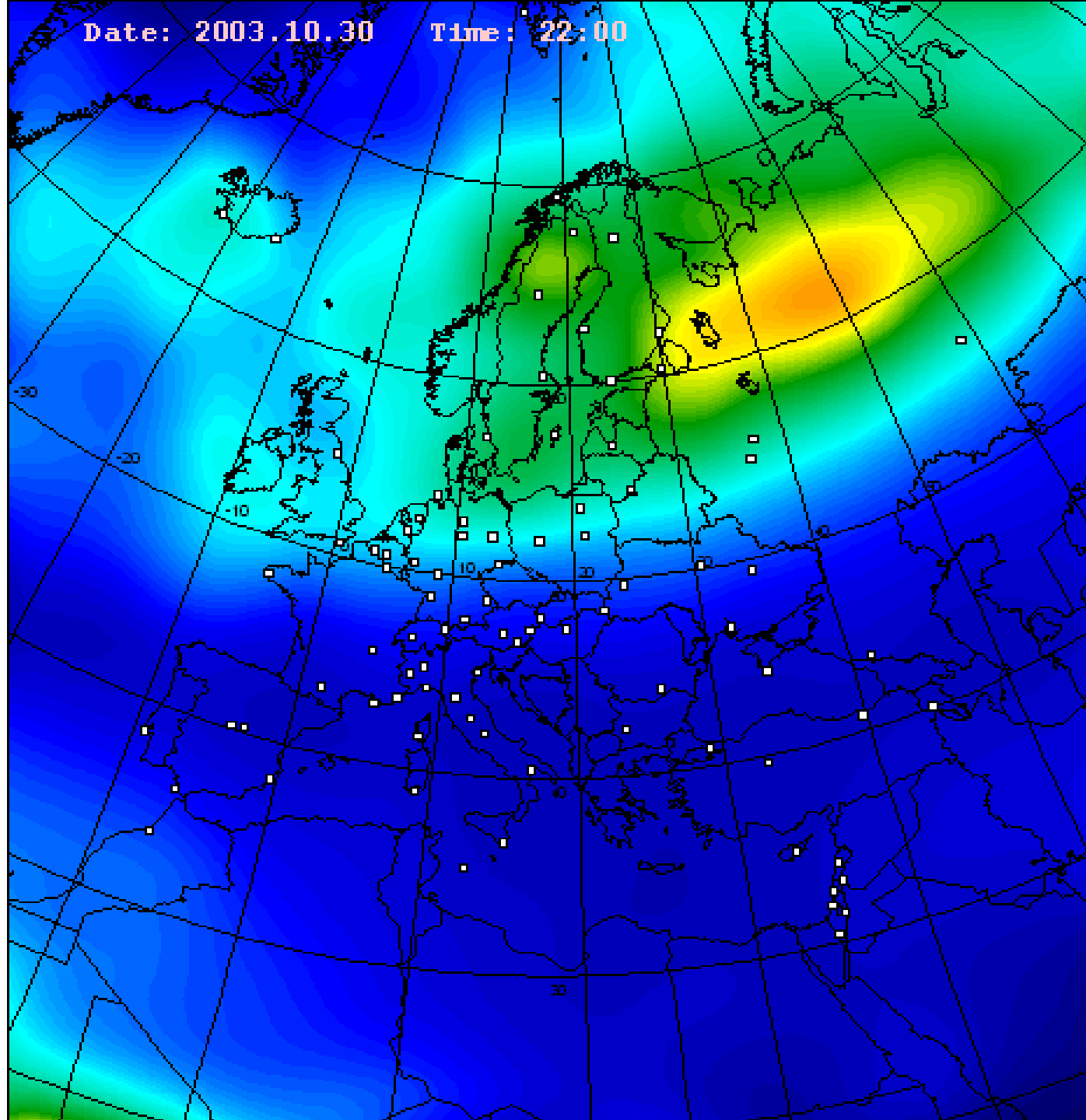
Date: 2003.10.30

Time: 21:00

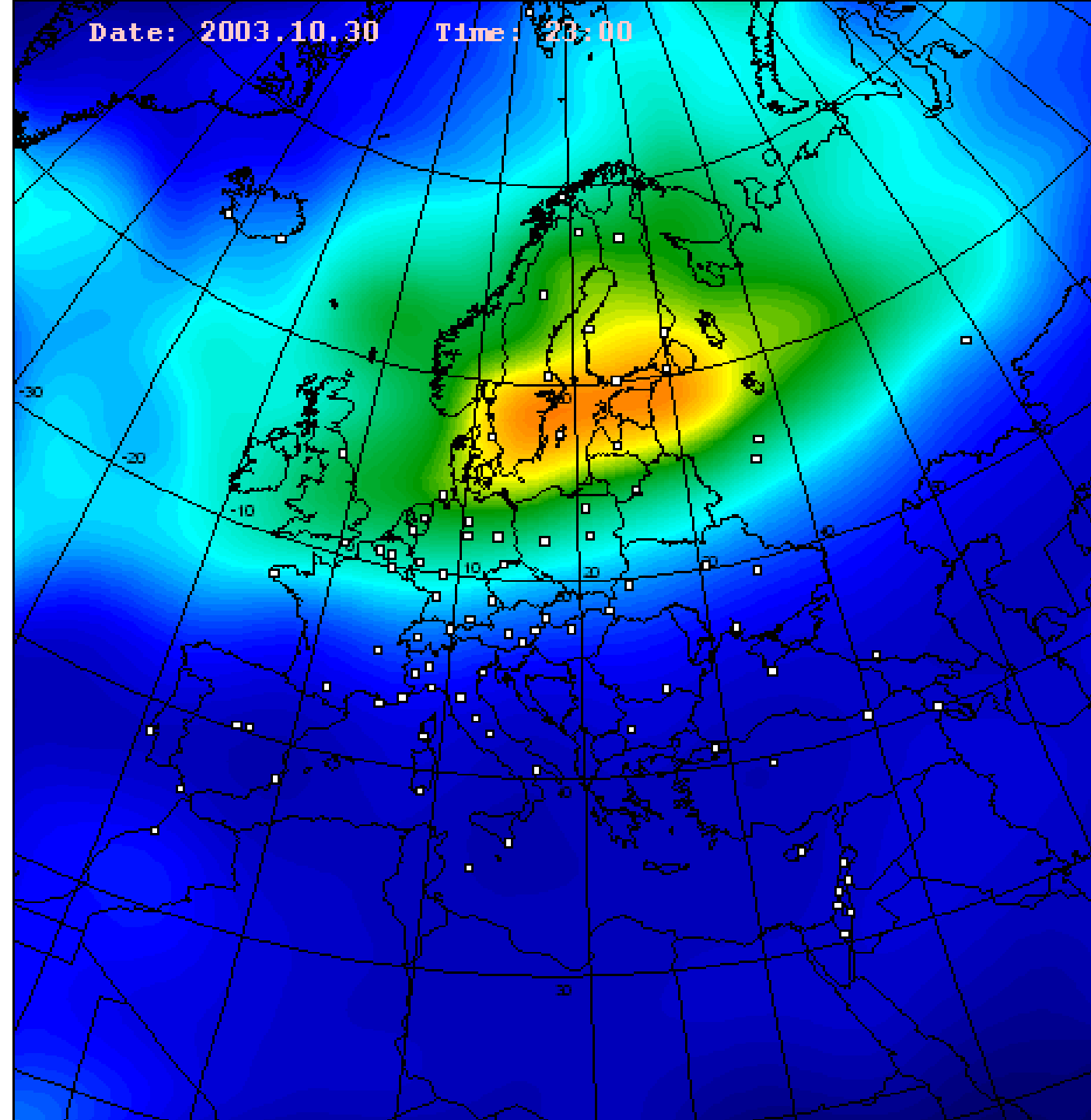


Date: 2003.10.30

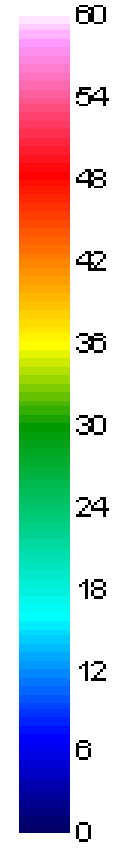
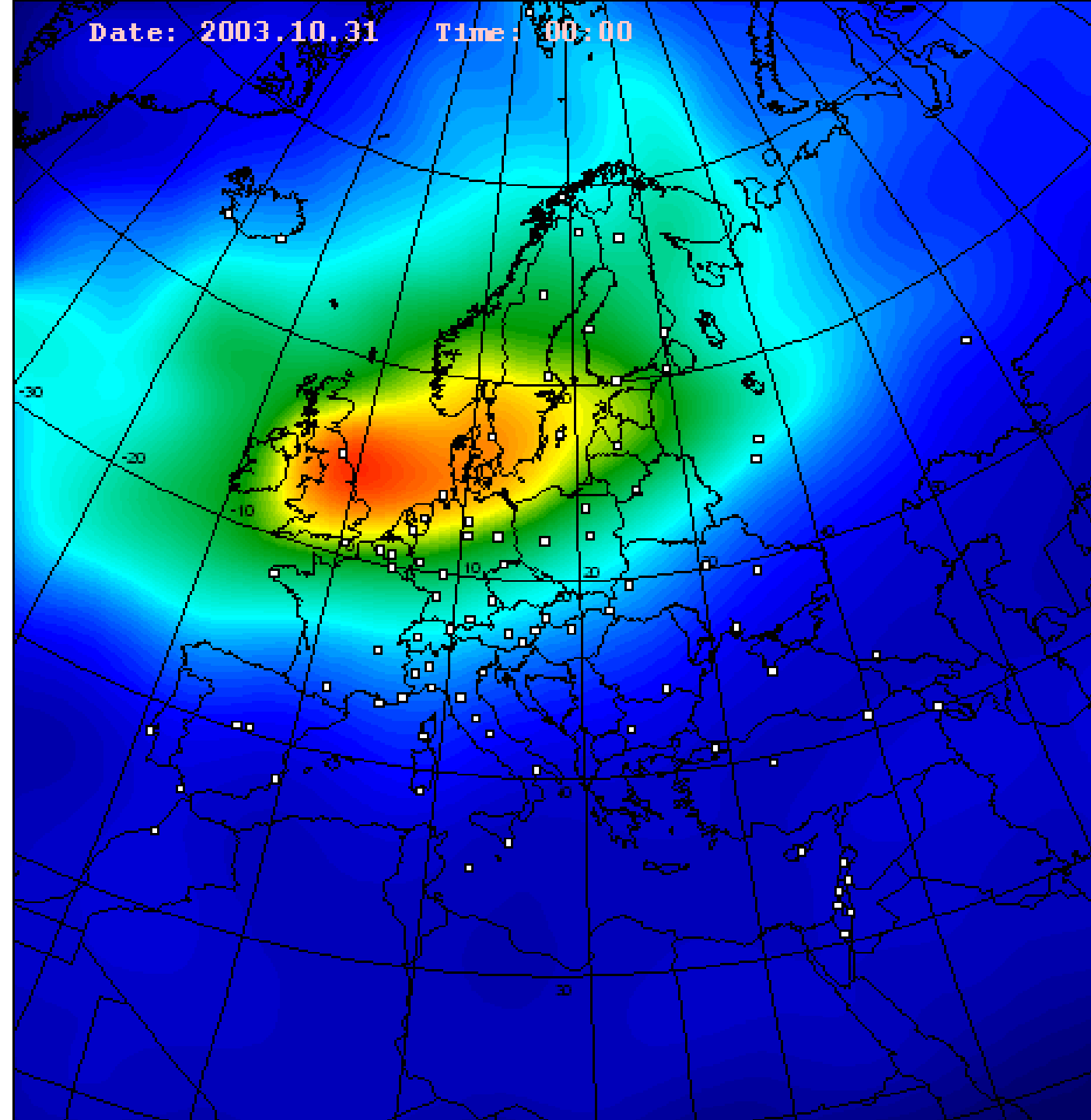
Time: 22:00



Date: 2003.10.30 Time: 23:00

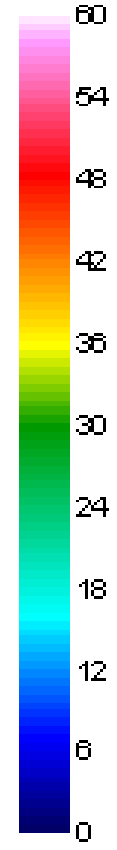
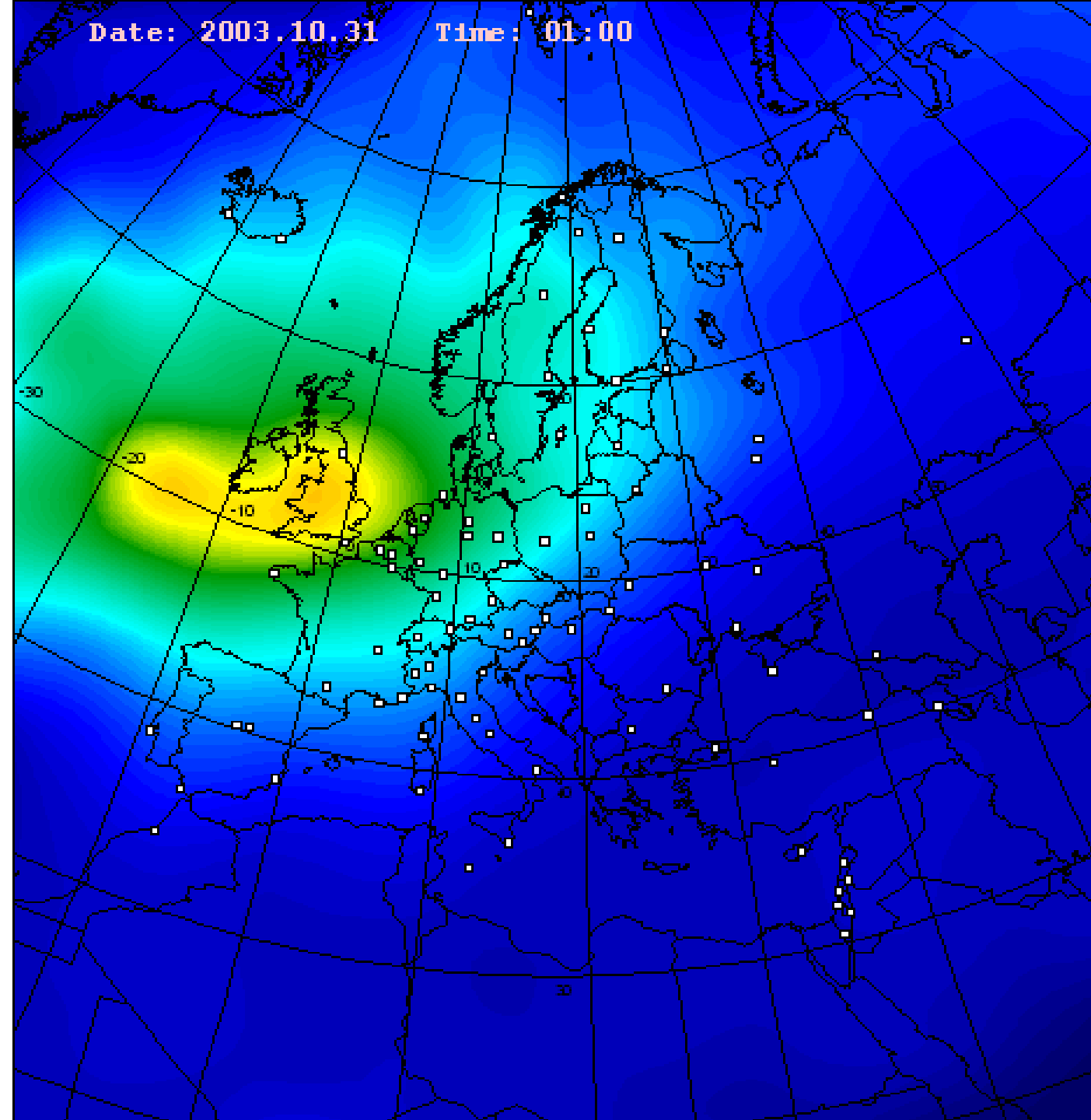


Date: 2003.10.31 Time: 00:00

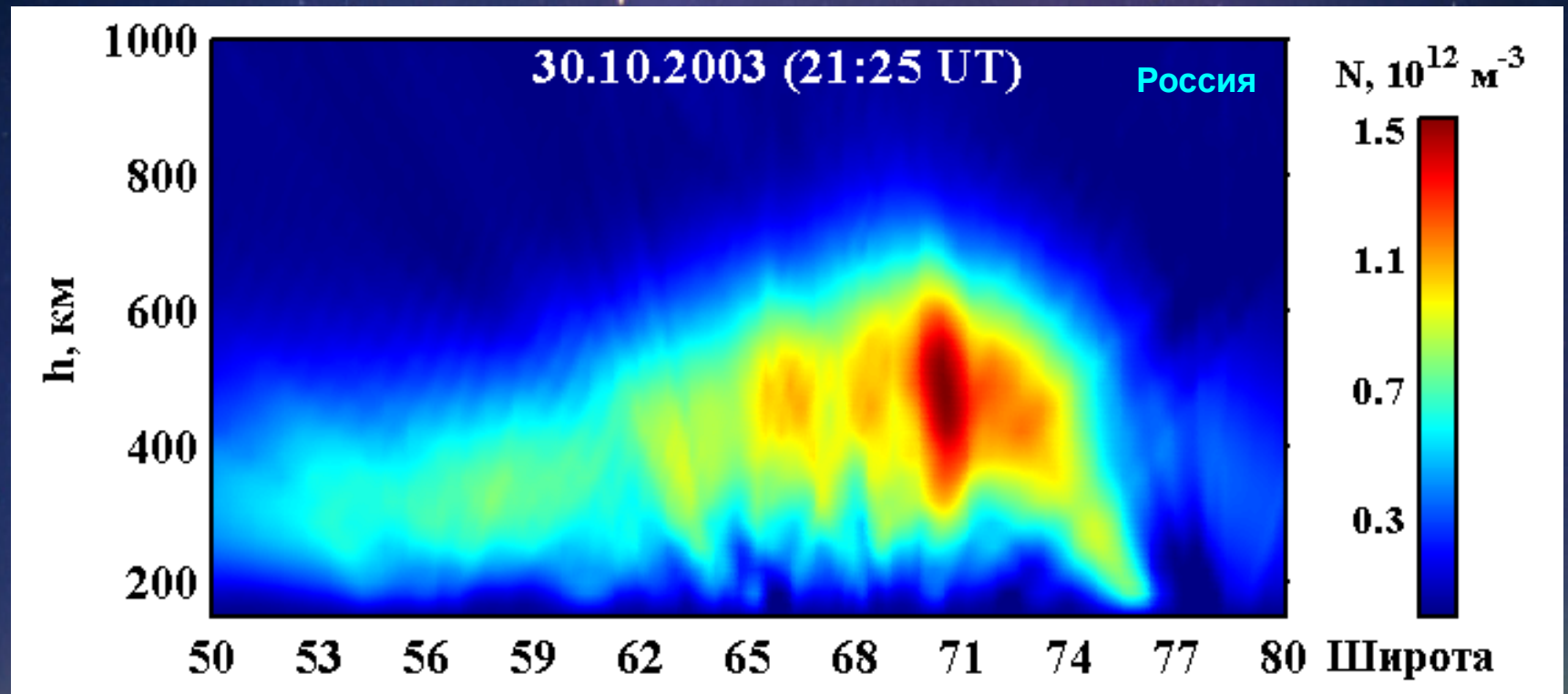


Date: 2003.10.31

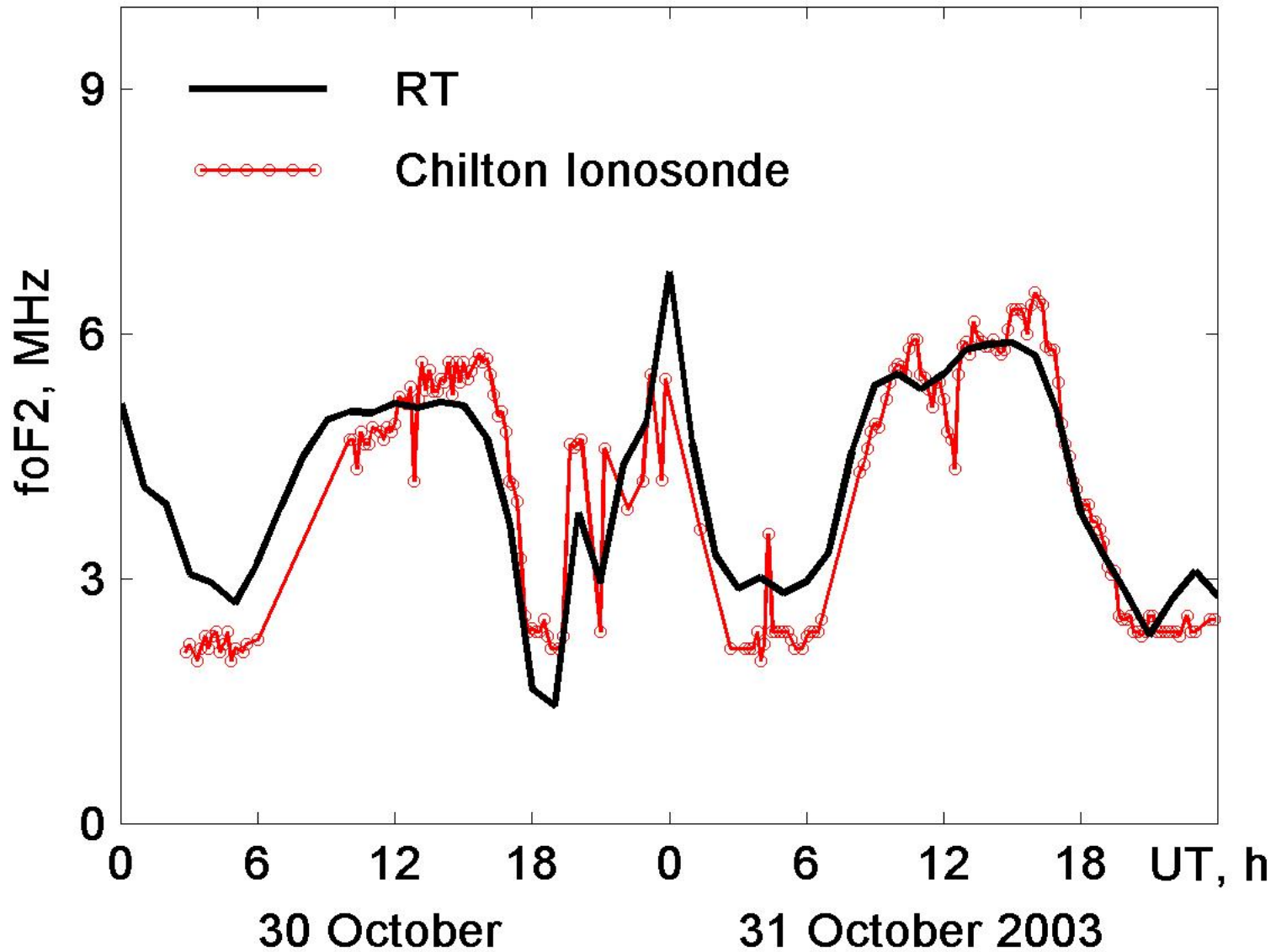
Time: 01:00



Solar Extreme Events of 2003

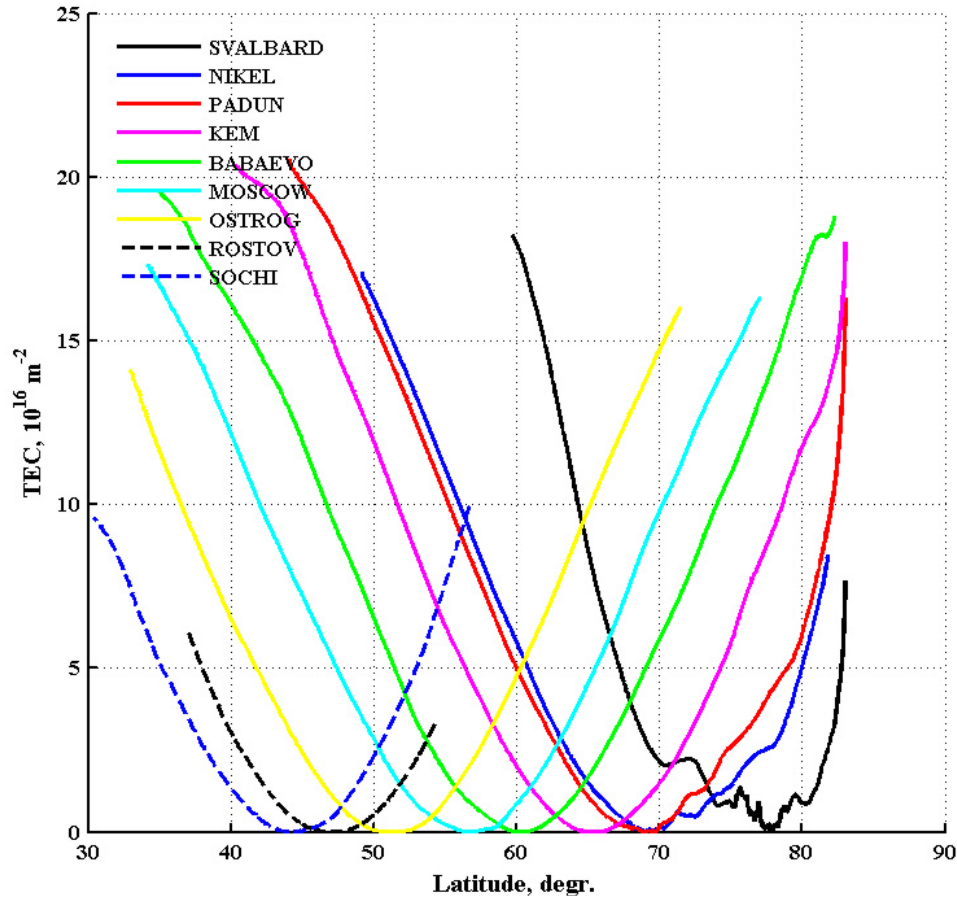


foF2 as obtained from RT and Chilton Ionosonde data



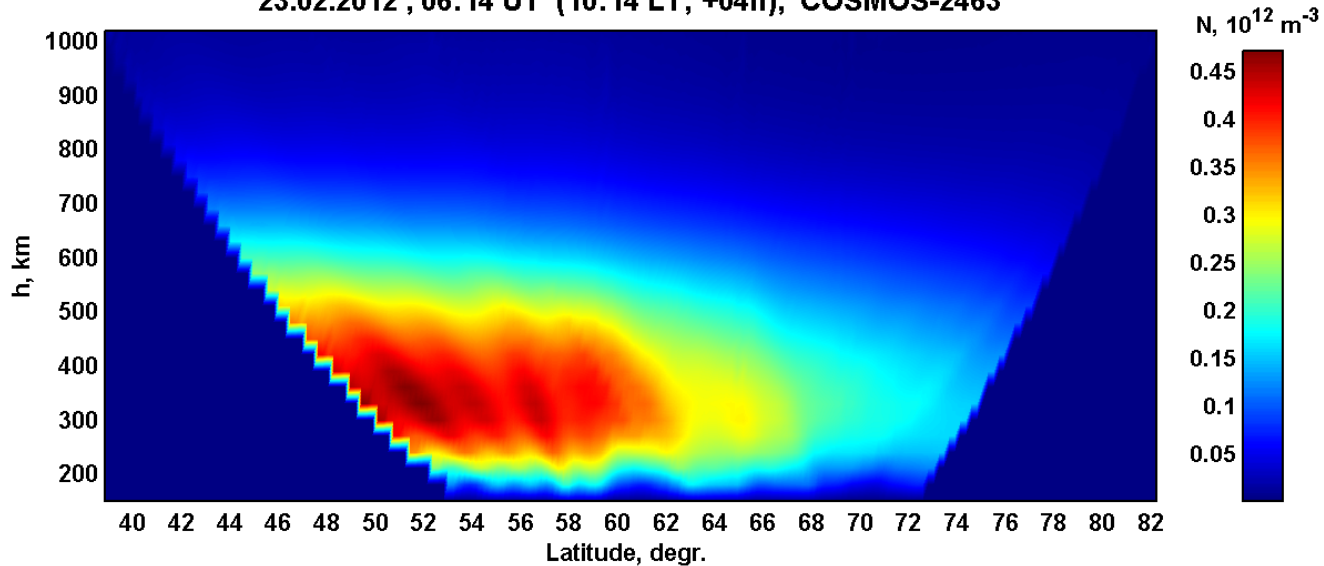
Russian LORT system (Svalbard – Moscow - Sochi)

31.08.2012 (17:27UT) COSMOS-2407



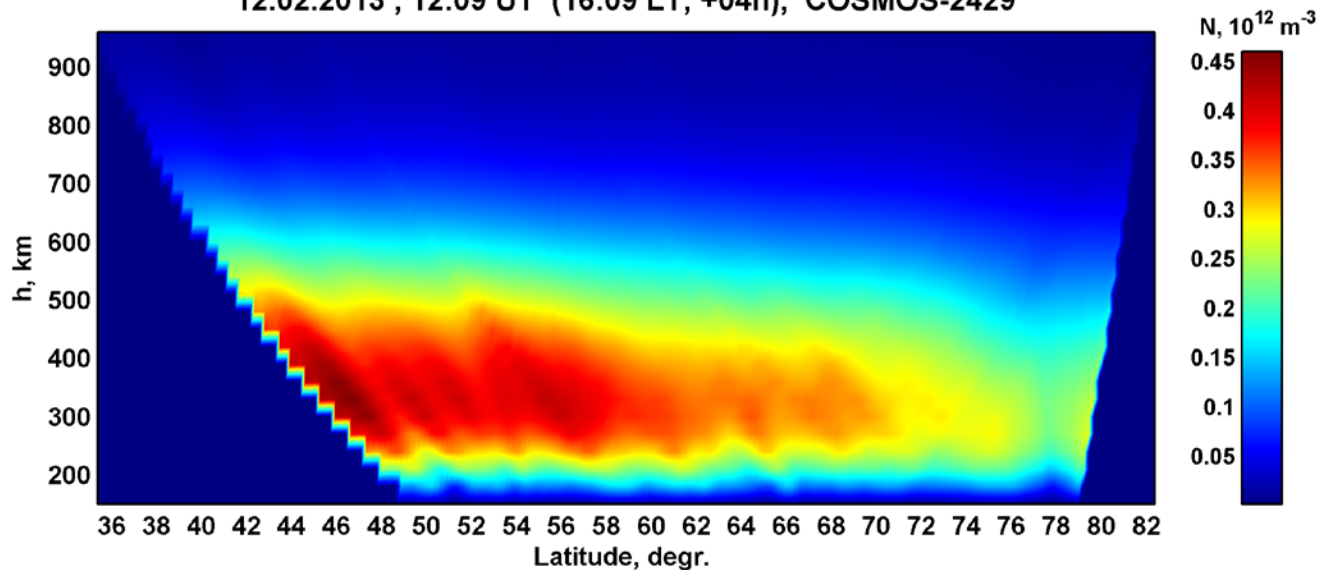
TIDs (Northwest of Russia)

23.02.2012 , 06:14 UT (10:14 LT; +04h), COSMOS-2463



LORT image above Russian RT chain on February 23, 2012 , 06:14 UT

12.02.2013 , 12:09 UT (16:09 LT; +04h), COSMOS-2429

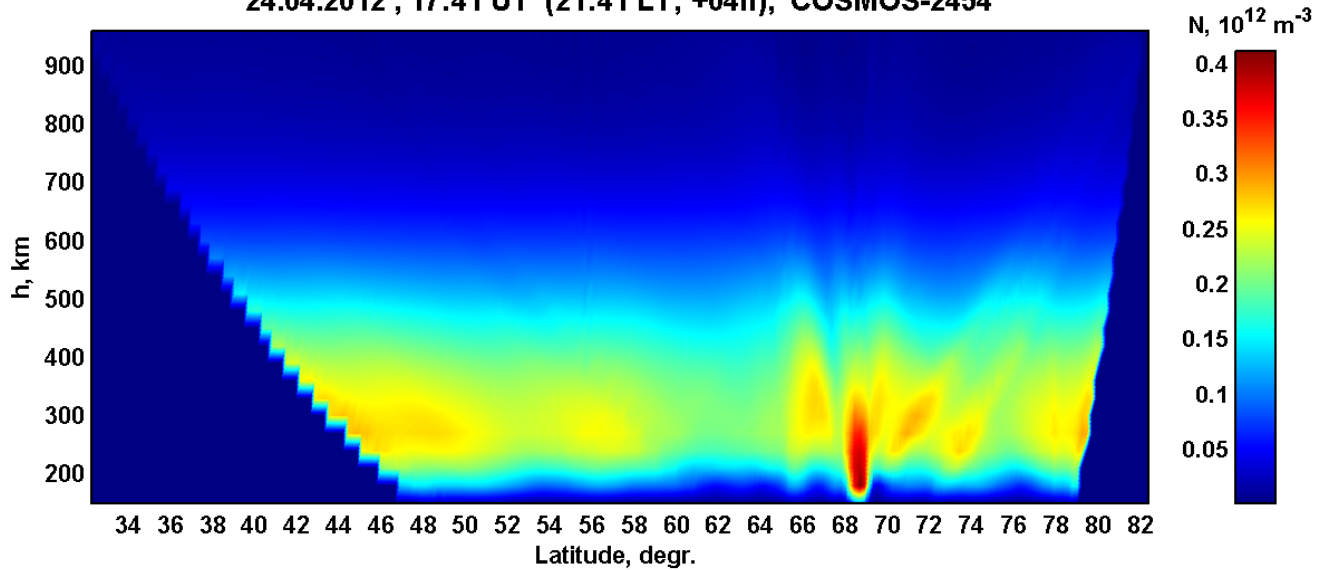


LORT image above Russian RT chain on February 12, 2013 , 12:09 UT

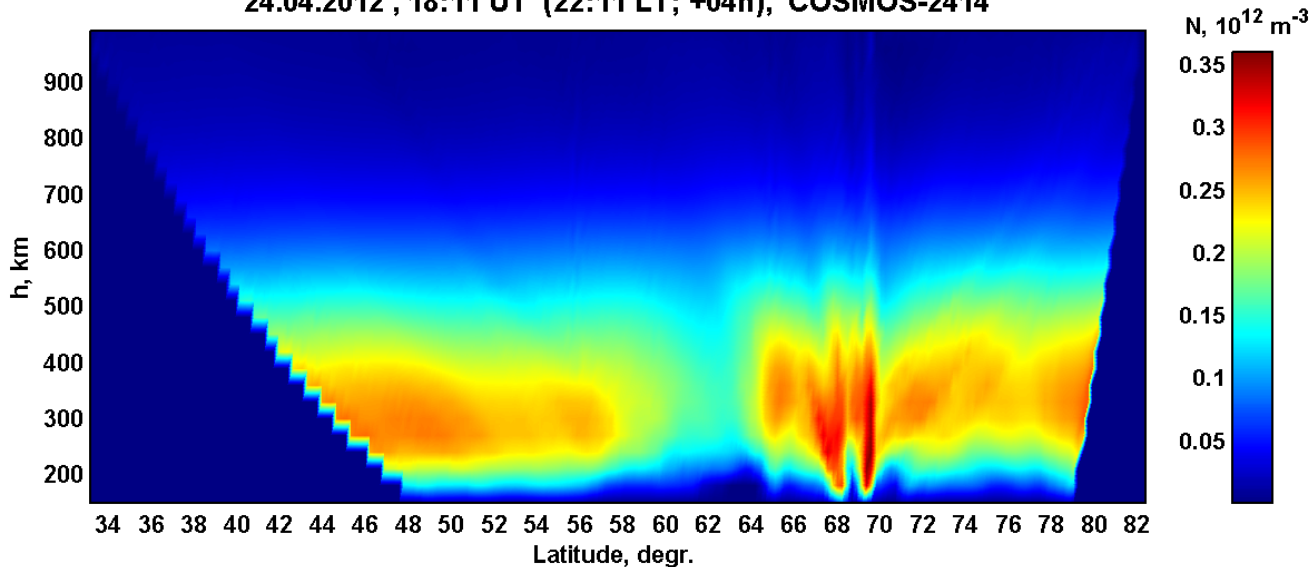
Region of Russian LORT system

ionospheric features are probably associated with particle precipitation

24.04.2012 , 17:41 UT (21:41 LT; +04h), COSMOS-2454

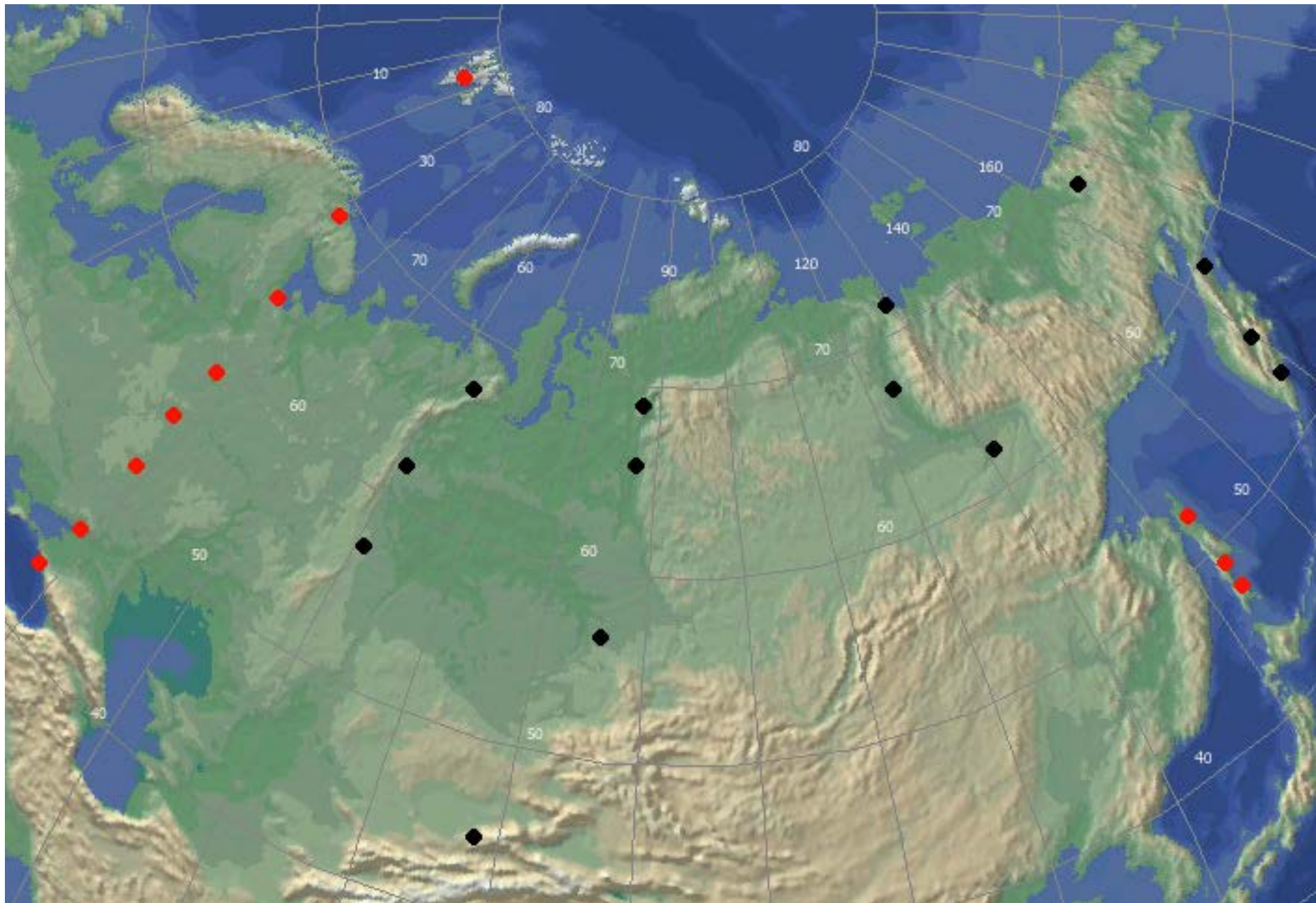


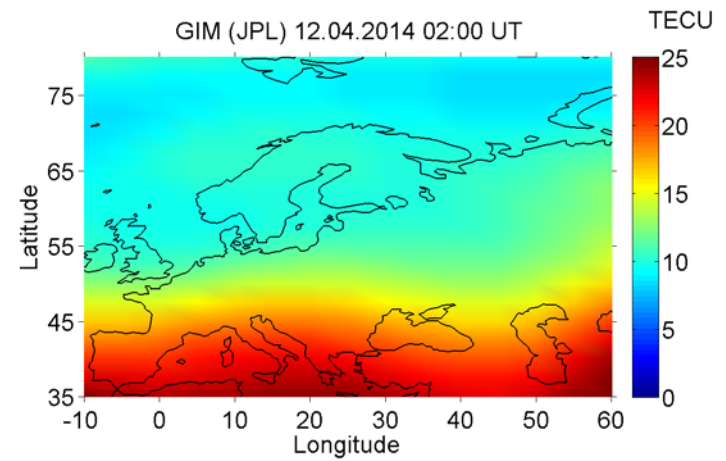
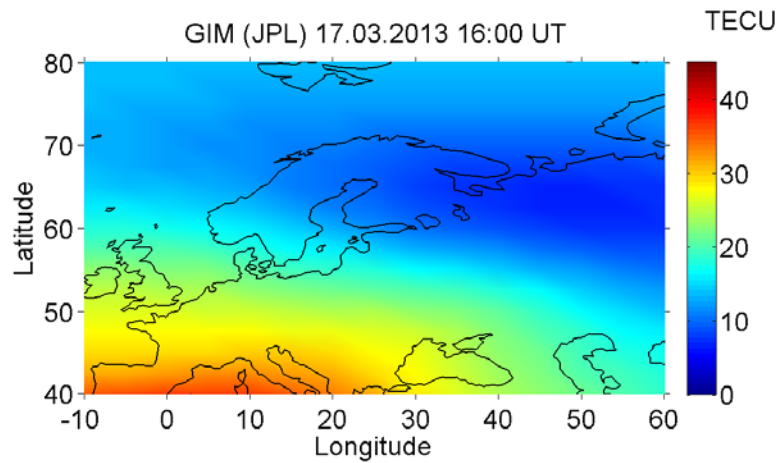
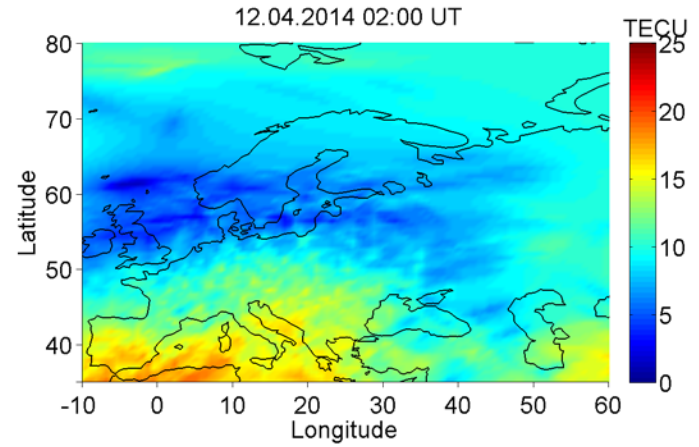
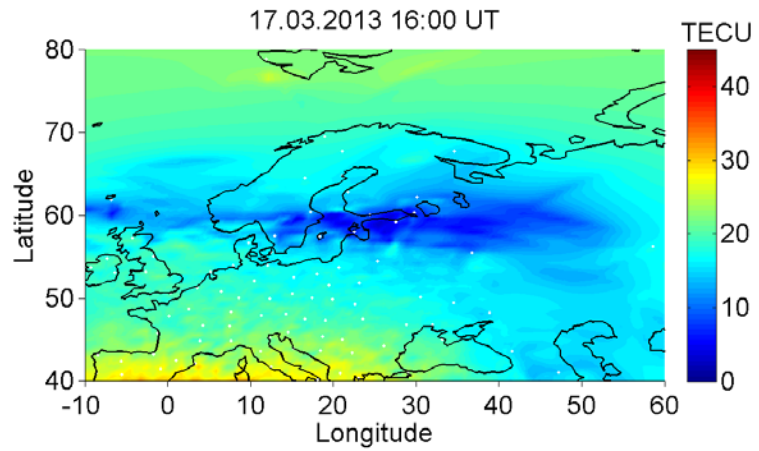
24.04.2012 , 18:11 UT (22:11 LT; +04h), COSMOS-2414

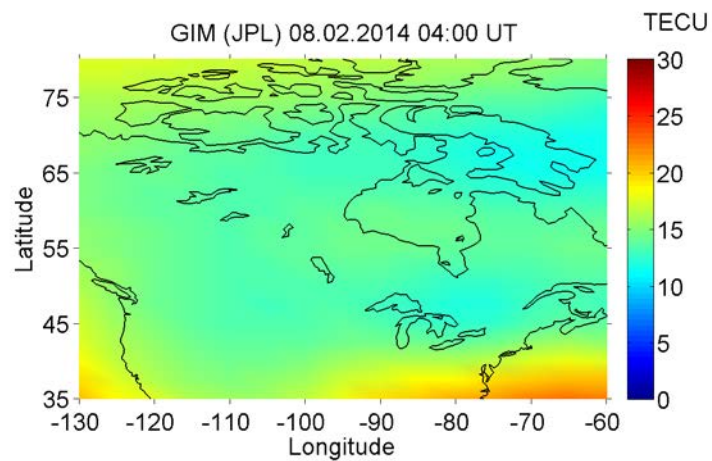
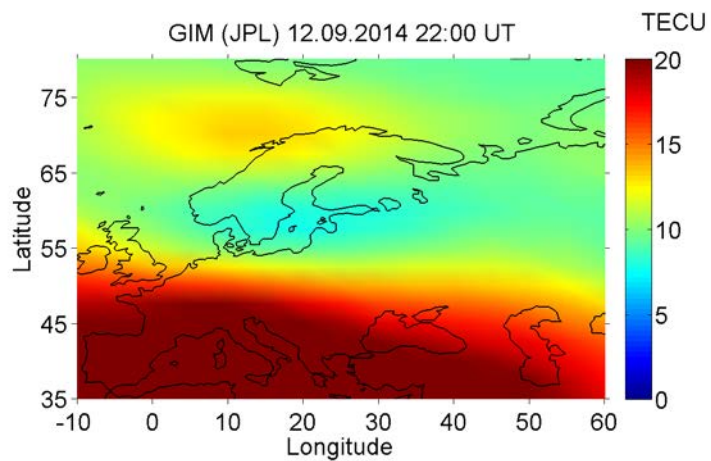
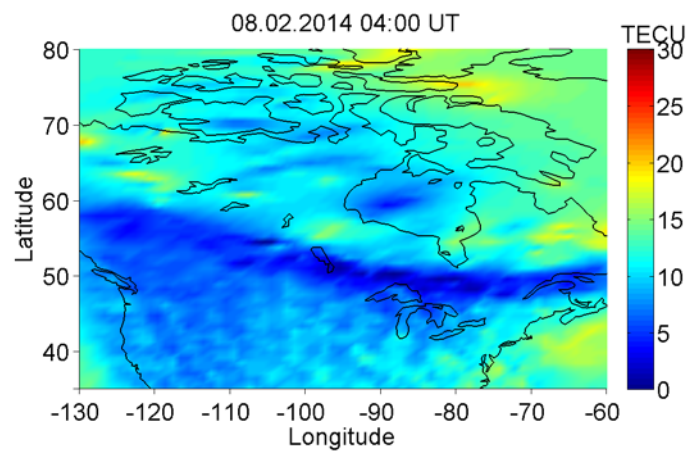
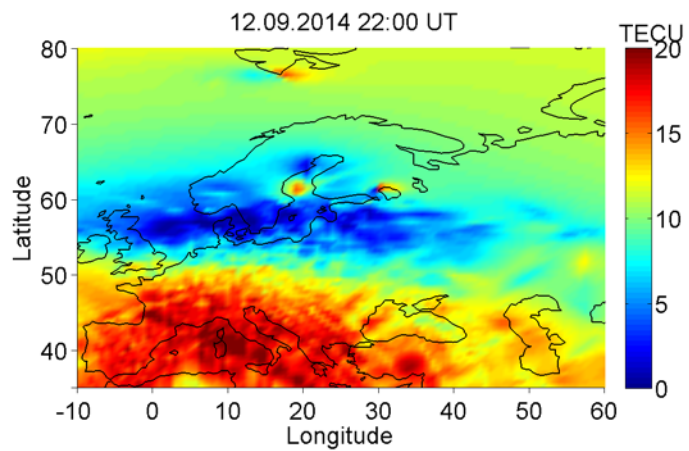


LORT images above Russian RT chain on April 24, 2012 , 17:41 and 18:11 UT

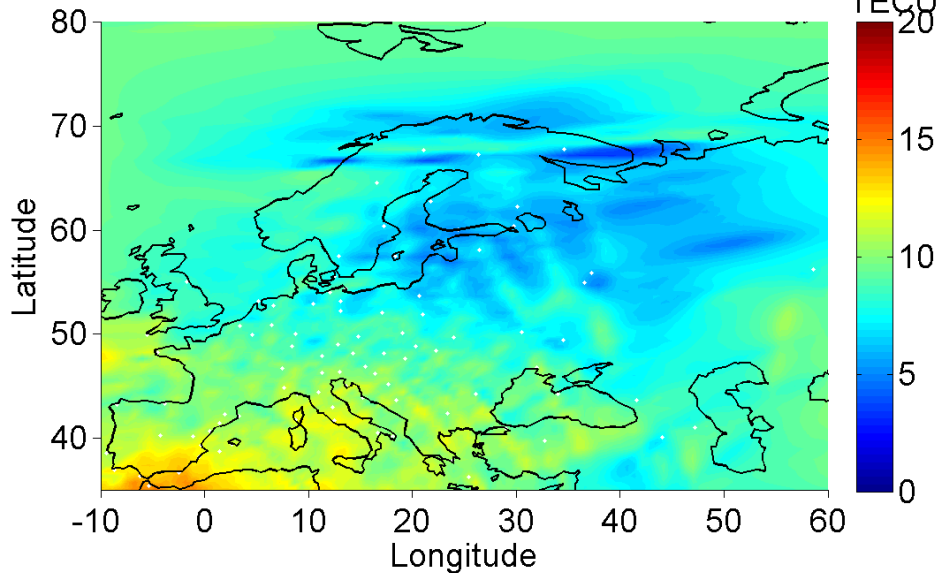
Система НОРТ. ФЦП “Создание системы мониторинга геофизической обстановки над территорией РФ на 2008-2015 годы”



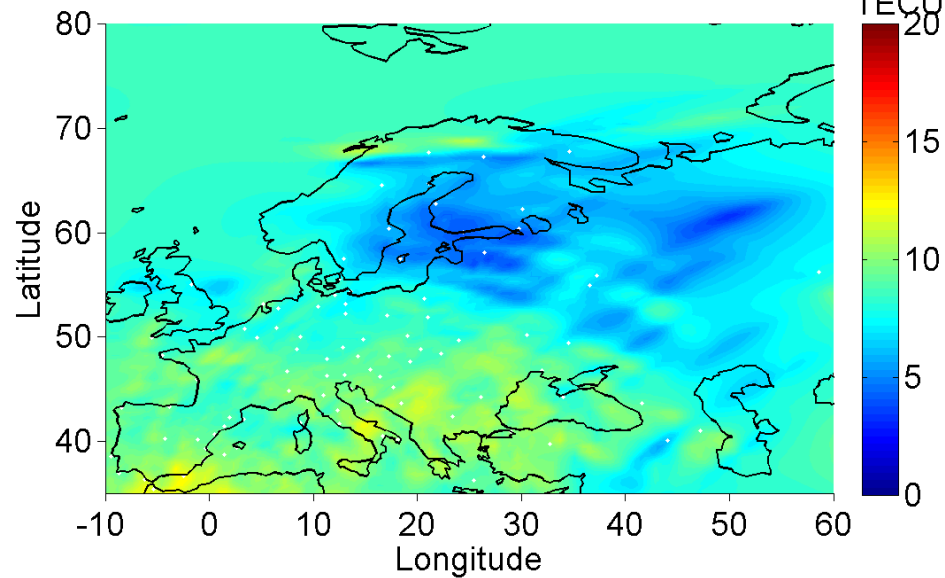




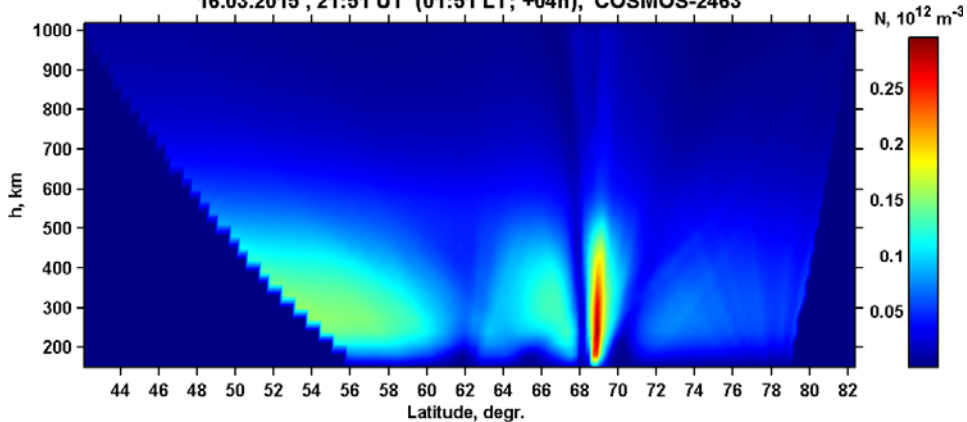
16.03.2015 22:00 UT



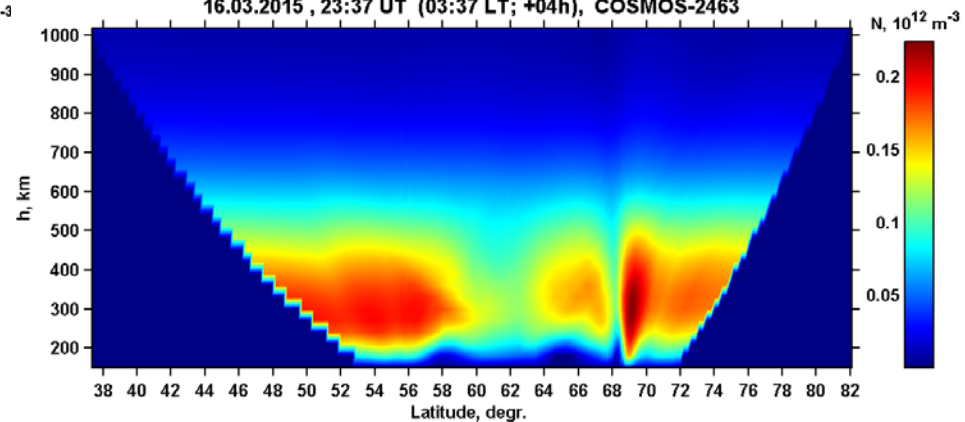
16.03.2015 23:00 UT

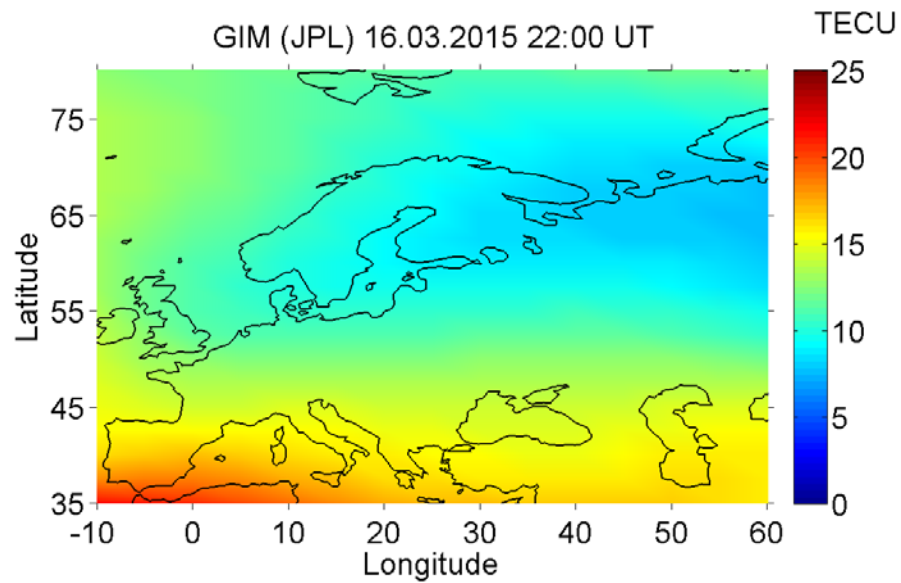
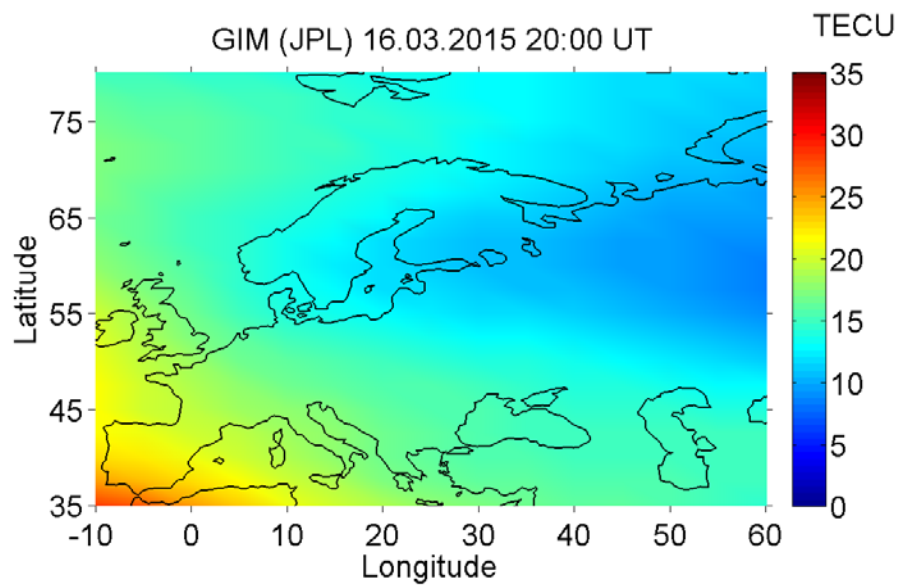
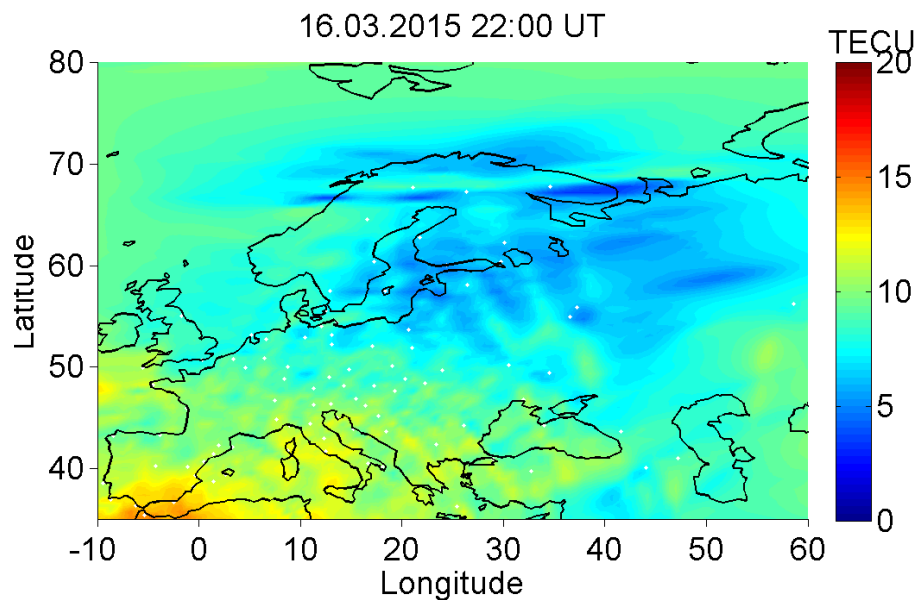
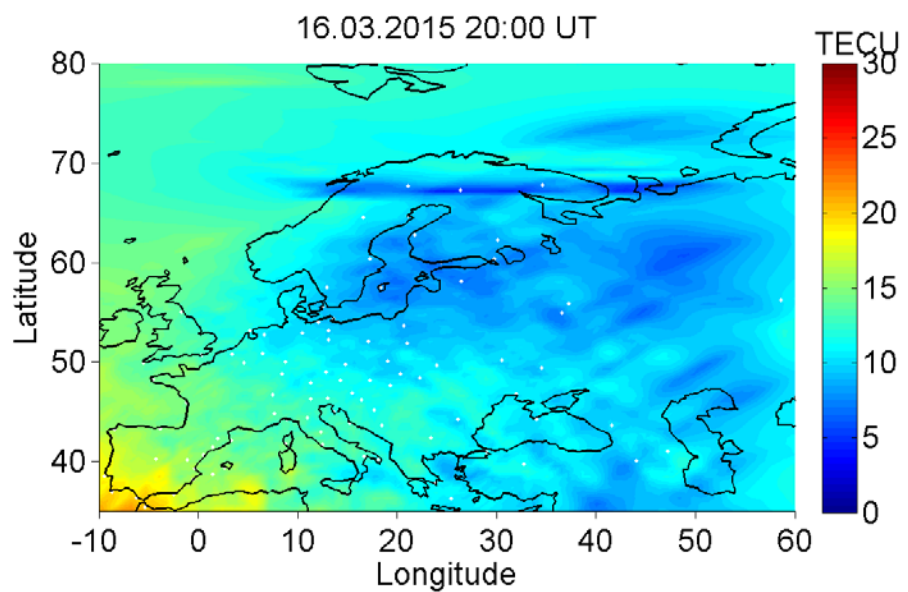


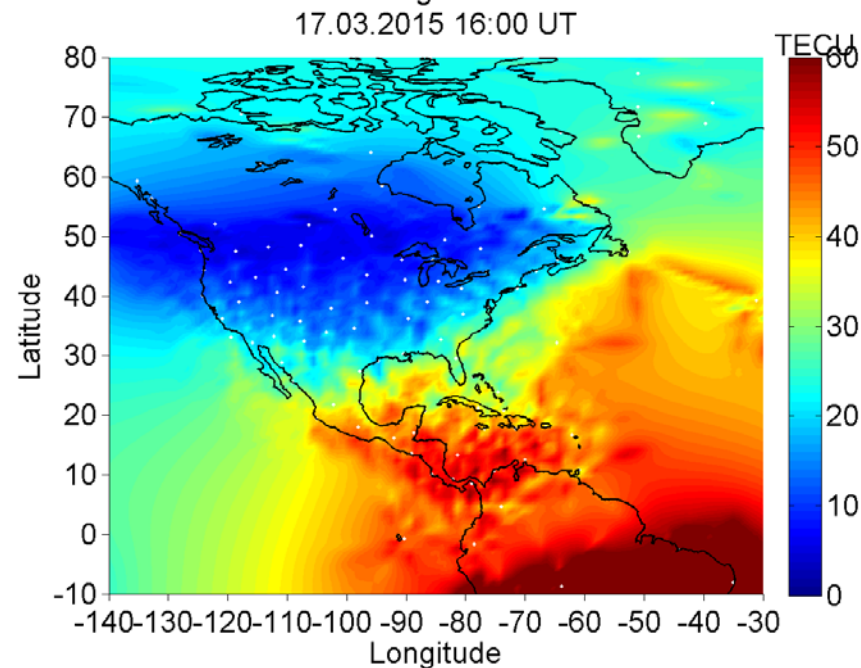
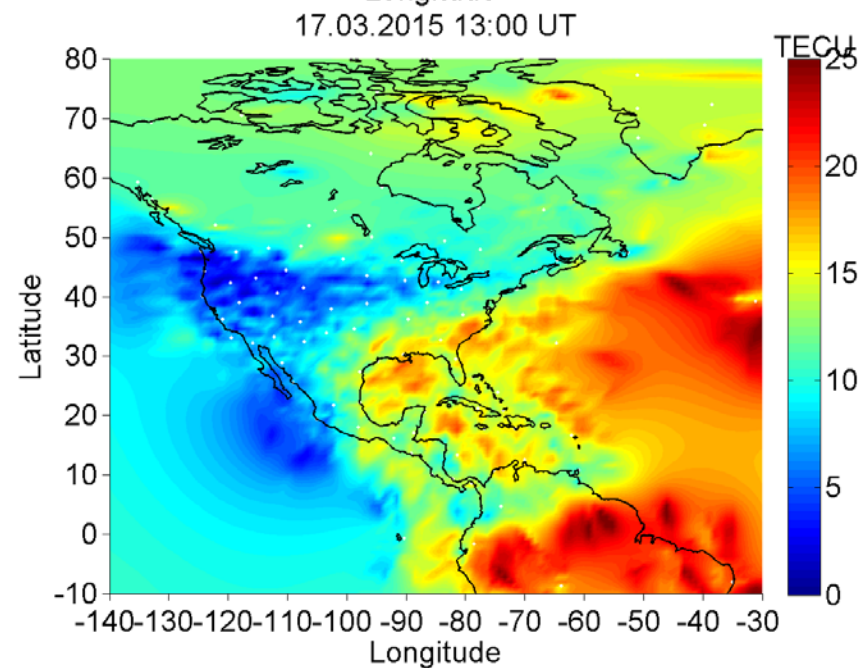
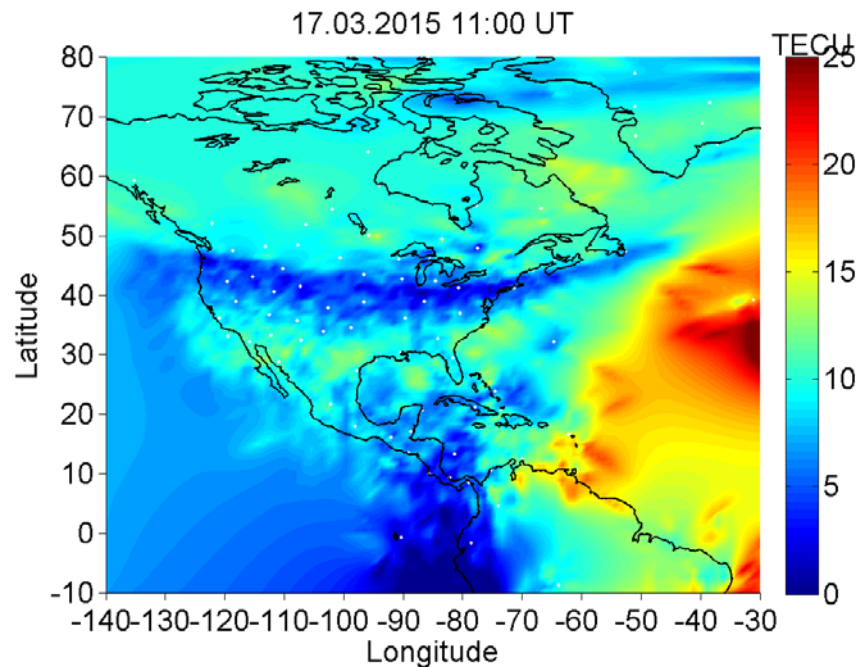
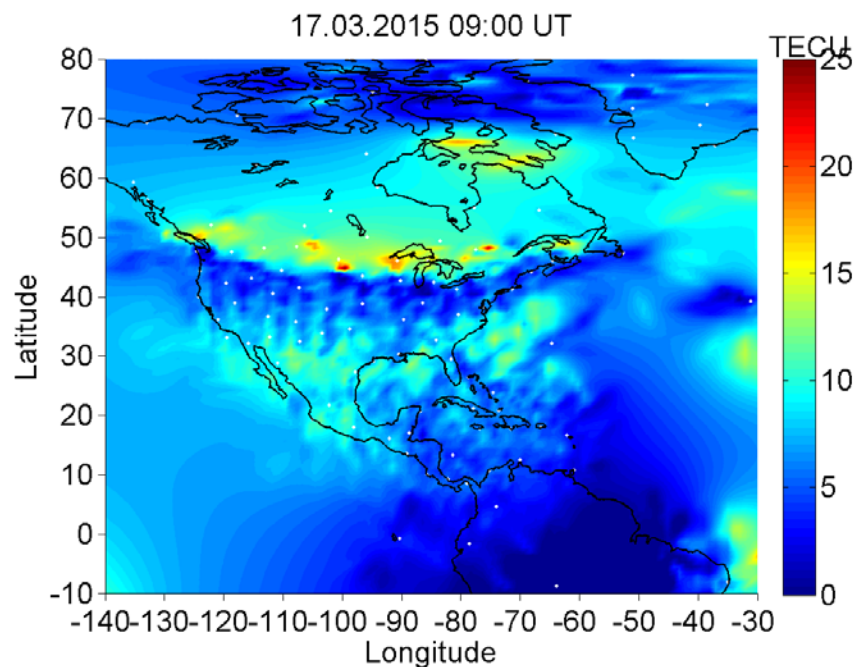
16.03.2015 , 21:51 UT (01:51 LT; +04h), COSMOS-2463



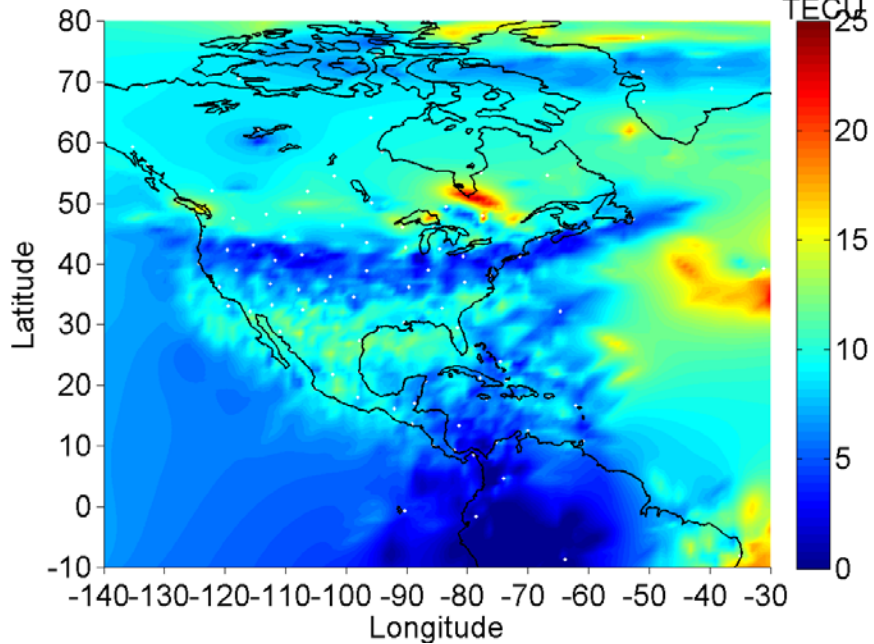
16.03.2015 , 23:37 UT (03:37 LT; +04h), COSMOS-2463



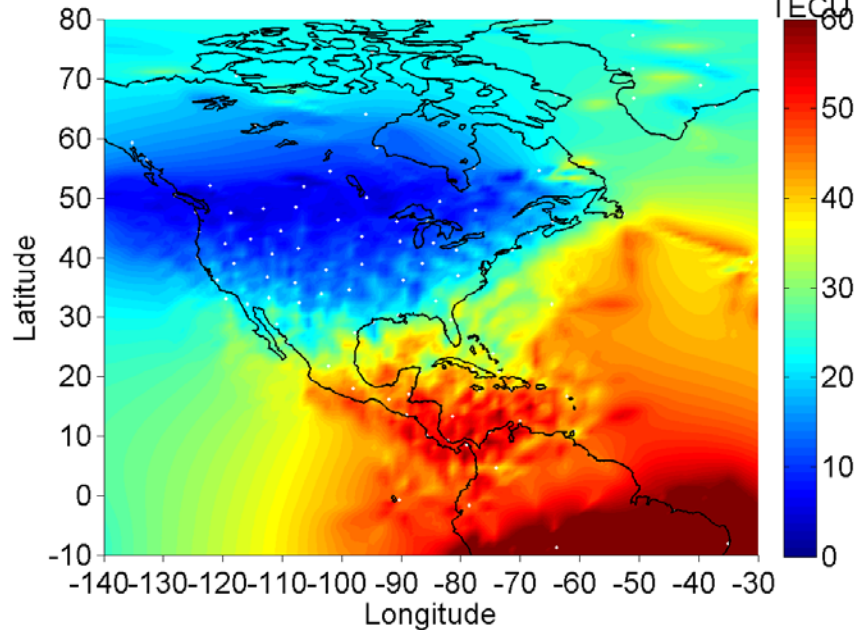




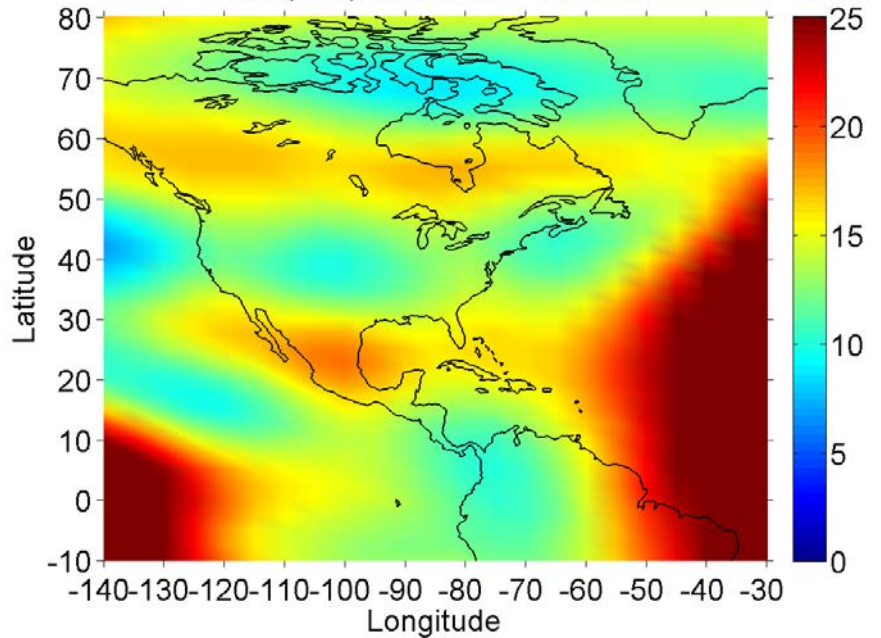
17.03.2015 10:00 UT



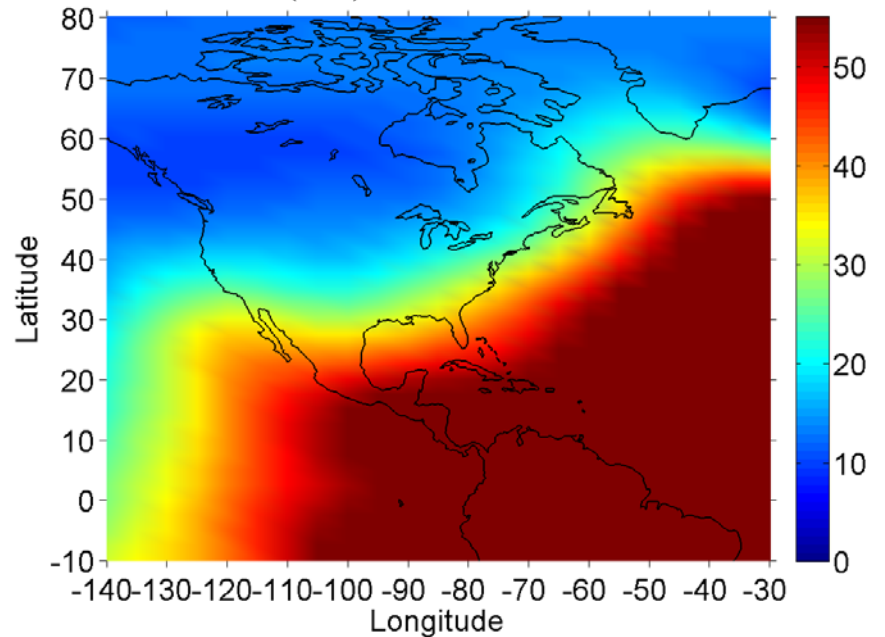
17.03.2015 16:00 UT



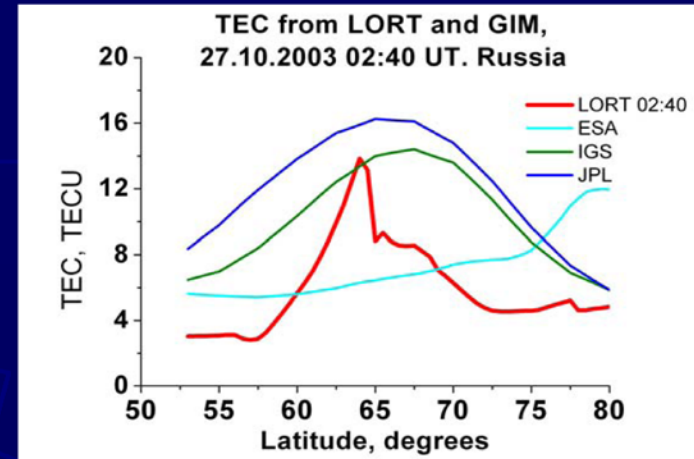
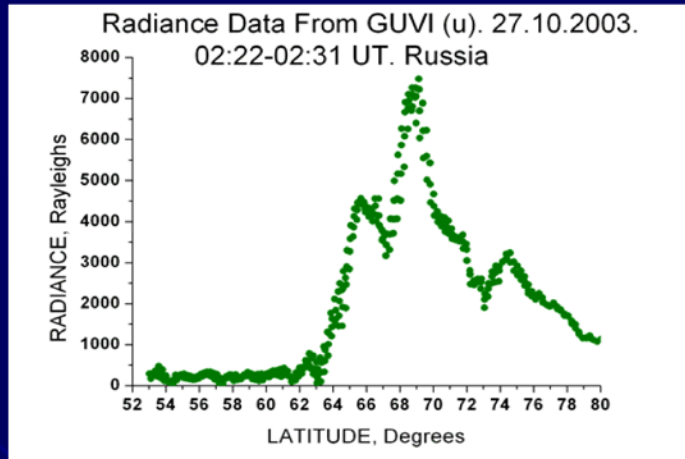
GIM (JPL) 17.03.2015 10:00 UT



GIM (JPL) 17.03.2015 16:00 UT



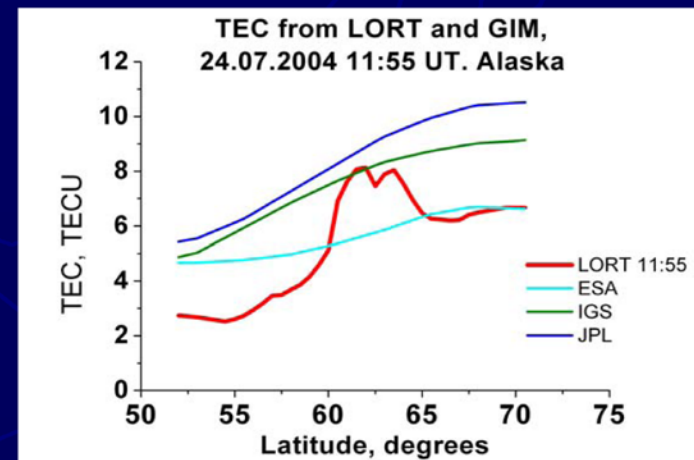
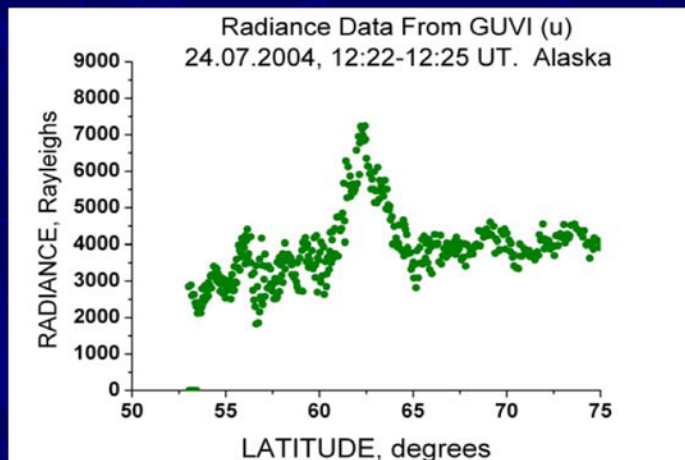
Comparison of GUVI Data and TEC by LORT and GIM



Dst=-47

Kp=3.3

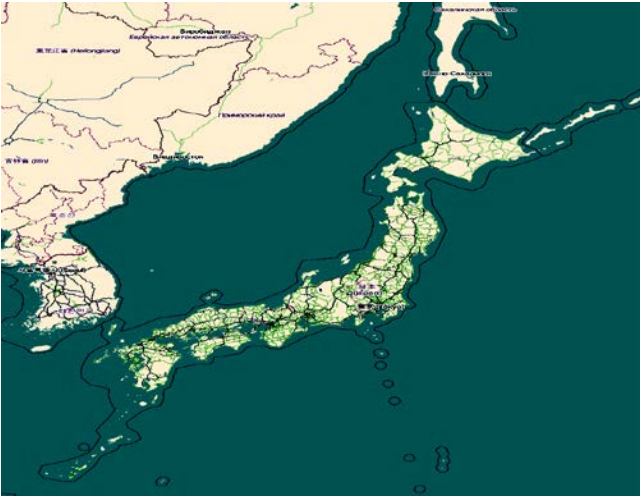
Ap=20



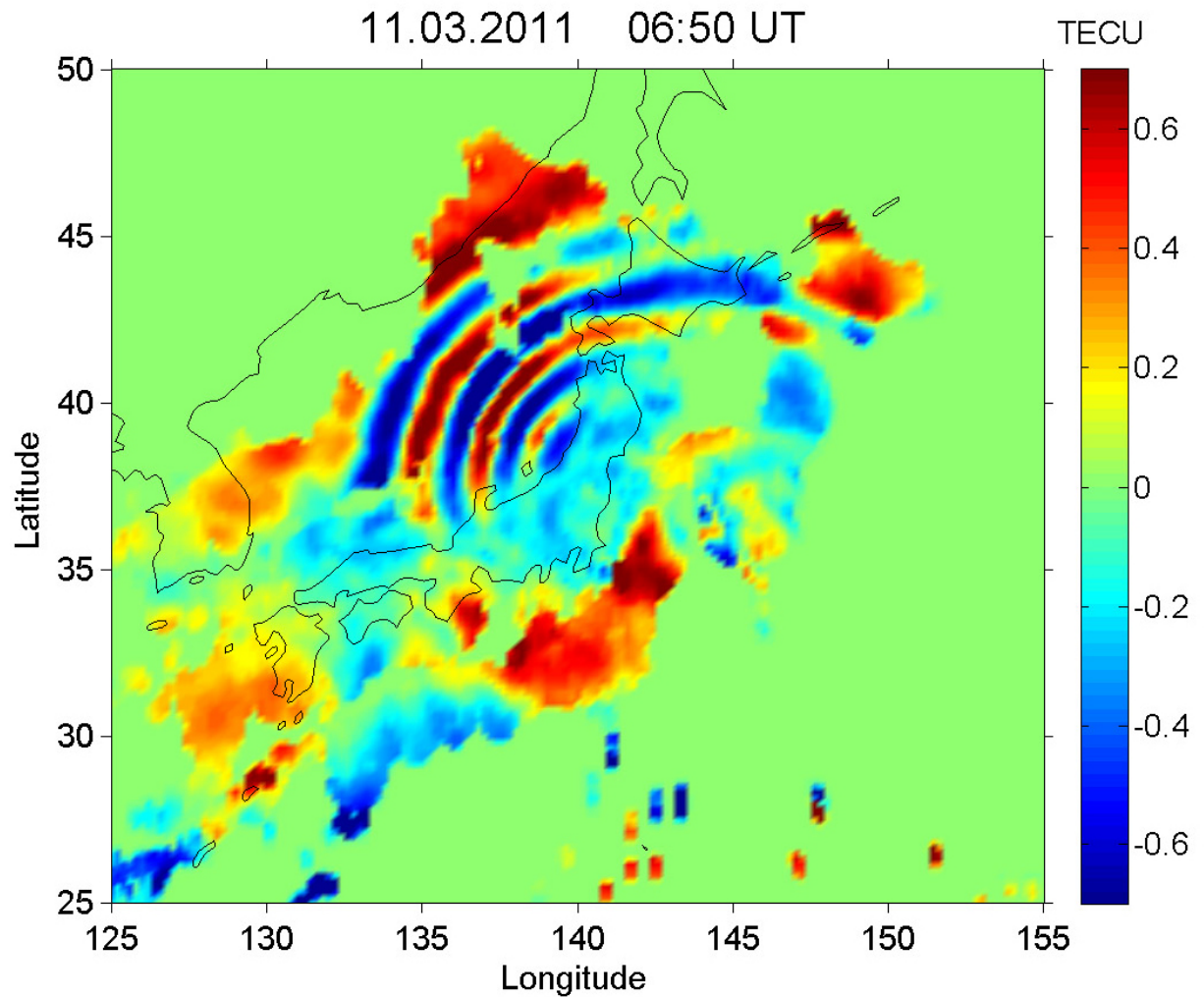
Dst=-18

Kp=6

Ap=80



Tohoku mega-earthquake



The TEC waves, caused by the AGW from the Tohoku mega-earthquake, diverging from the epicenter of the event.

SUMMARY

- The combination of LORT and HORT systems provides significant advantages: HORT yields 3D distributions of the ionospheric plasma over vast regions, and LORT provides significantly higher resolution.
- The existing systems implementing the radio occultation (RO) approach (FormoSat-3/COSMIC and other systems that record the signals from the GPS/GLONASS satellites at HO satellites) provide the quasi tangential projections of electron density N .

The combination of the RT and RO methods, which supports the RT data by the probing data on the satellite-to-satellite paths (RO data), can significantly improve vertical resolution of RT reconstructions.

- The existing UV sounder systems (GUVI, SSULI) provide the integrals of N squared. In this case, the data from UV sounders can be incorporated into the common tomographic iterative scheme; however, the data should be consistent in terms of accuracy.
- GIM TEC data are generally smoother than the results provided by RT. The GIM TEC data during the severe geomagnetic disturbances should be used with caution.

ACKNOWLEDGEMENTS

We are grateful to the NWRA for providing the data from Alaska RT System and Taiwan National Central University for providing the data from Taiwan RT System and Radio-Hydro-Physics LLC for providing the data from West Coast US RT System . The GIM data were obtained through <ftp://ftp.unibe.ch/aiub/> CODE/.